Atmos. Chem. Phys. Discuss., 5, 12255–12311, 2005
www.atmos-chem-phys.org/acpd/5/12255/
SRef-ID: 1680-7375/acpd/2005-5-12255
European Geosciences Union

Atmospheric Chemistry and Physics Discussions

Impact of aircraft NO_x emissions on the atmosphere – tradeoffs to reduce the impact

M. Gauss[1], I. S. A. Isaksen[1], D. S. Lee[2], and O. A. Søvde[1]

[1]Department of Geosciences, University of Oslo, Oslo, Norway
[2]Centre for Air Transport and the Environment, Manchester Metropolitan University, Manchester, UK

Received: 26 October 2005 – Accepted: 15 November 2005 – Published: 25 November 2005

Correspondence to: M. Gauss (michael.gauss@geo.uio.no)

Abstract

Within the EU-project TRADEOFF, the impact of NO_x (=NO+NO_2) emissions from subsonic aviation upon the chemical composition of the atmosphere has been calculated with focus on changes in reactive nitrogen, ozone, and the chemical lifetime of methane. We apply a 3-D chemical transport model that includes comprehensive chemistry for both the troposphere and the stratosphere and uses various aircraft emission scenarios developed during TRADEOFF for the year 2000. The environmental effects of enhanced air traffic along polar routes and of possible changes in cruising altitude are investigated.

In the reference case the model predicts aircraft-induced maximum increases of zonal-mean NO_y (=total reactive nitrogen) between 156 pptv (August) and 322 pptv (May) in the tropopause region of the Northern Hemisphere. Resulting maximum increases in zonal-mean ozone vary between 3.1 ppbv in September and 7.7 ppbv in June. The lifetime of methane is calculated to decrease by 0.71%, inducing a radiative forcing of $-6.4\,mW/m^2$.

Enhanced use of polar routes implies significantly larger zonal-mean ozone increases in high Northern latitudes during summer, while the effect is negligible in winter.

Lowering the flight altitude leads to smaller ozone increase in the lower stratosphere and upper troposphere, and to larger ozone increase at lower altitudes. Regarding total ozone change, the degree of cancellation between these two effects depends on latitude and season, but annually and globally averaged the stratospheric decrease dominates, mainly due to washout of NO_y in the troposphere, which weakens the tropospheric increase.

Raising flight altitudes increases the ozone burden both in the troposphere and the lower stratosphere, primarily due to a more efficient accumulation of pollutants in the stratosphere.

ACPD

5, 12255–12311, 2005

1. Introduction

Driven mainly by continuing economic growth and reduced fares, passenger traffic is estimated to grow at an average annual rate of nearly 5 percent during the period 2001–2020 (Airbus Global Market Forecast, 2002), making civil aviation one of the fastest growing industrial sectors. Emissions of aircraft include carbon dioxide (CO_2), water vapor (H_2O), nitric oxide (NO), nitrogen dioxide (NO_2), carbon monoxide (CO), a variety of hydrocarbons (HC), sulfur oxides, soot and other particles. Different aspects of the impact of aircraft emissions on the atmosphere have been identified, including changes in greenhouse gases, particles, contrails, and cirrus cloud formation (e.g. Fabian and Kärcher, 1997; Brasseur et al., 1998; Penner et al., 1999; Schumann et al., 2000; Isaksen et al., 2003). The main threat of aviation to the wider environment is believed to lie in its contribution to climate change.

The present study deals with the impact of NO_x emissions from aircraft, which, although representing only 1–2% of the total emissions of NO_x from man-made and natural sources in the early 1990s (Lee et al., 1997), may have a pronounced impact on the chemical composition of the atmosphere. During the last three decades numerous studies have focused on the different implications of NO_x emissions from aircraft (e.g. Hidalgo and Crutzen, 1977; Johnson et al., 1992; Schumann et al., 1997; Dameris et al., 1998; Kentarchos and Roelofs, 2002; Grewe et al., 2002a, b). Most importantly, NO_x emissions from aircraft are expected to increase ozone in the upper troposphere and lower stratosphere region (UTLS).

In contrast to all other major anthropogenic emission sources, aircraft emit their exhaust products directly into the UTLS, where pollutants have a much longer lifetime than at Earth's surface, allowing excess nitric oxide and ozone to accumulate to larger and more persistent perturbations than at Earth's surface. These factors, combined with the relatively large radiative forcing caused by ozone increases occurring in the UTLS (Wang and Sze, 1980; Lacis et al., 1990; Hansen et al., 1997), make aircraft NO_x emissions disproportionately important to the total O_3 radiative forcing from all

ACPD
5, 12255–12311, 2005

sources. On the other hand, additional NO_x and ozone enhance the concentration of the hydroxyl radical (OH), whereby the chemical lifetime of methane (CH_4), which is lost primarily through the reaction with OH, is reduced. The degree, to which the positive radiative forcing from ozone increases and the negative radiative forcing from methane reductions cancel each other, has long been under investigation (Penner et al., 1999). It is clear, however, that the two effects cannot be easily compared as they act on spatially different scales (Isaksen et al., 2001). Due to the relatively long lifetime of methane its aircraft-induced increases are well-mixed throughout the globe and exert radiative forcing mainly in low and mid latitudes. Ozone, on the other hand, is a short-lived greenhouse gas, with the largest perturbations and concomitant radiative forcing near the aircraft emission source in high northern latitudes.

The implication of NO_x emissions for ozone levels depends strongly on the altitude of the emissions for both chemical and dynamical reasons. As aircraft emissions occur near the tropopause, only small shifts in flight altitude will lead to large changes in the fraction of emissions released into the stratosphere, where pollutants accumulate more efficiently due to less vertical mixing and the absence of washout processes. Secondly, the chemical production of ozone per emitted NO_x molecule is a non-linear function of ambient levels of NO_x (Brasseur et al., 1998; Jaeglé et al., 1998, 1999) and the availability of hydrocarbons (Brühl et al., 2000; Kentarchos and Roelofs, 2002), which in turn largely depend on altitude. In the sunlit troposphere and lower stratosphere, NO_x leads to efficient ozone production through oxidation of carbon monoxide, methane, and higher hydrocarbons. At higher altitudes in the stratosphere this source becomes less important due the limited availability of hydrocarbons, while catalytic ozone depletion cycles involving NO_x (Crutzen, 1970; Johnston, 1971) gain importance, and the injection of NO_x actually destroys ozone rather than producing it.

The study presented in this paper has been performed within the EU-project TRADEOFF, funded by Framework Programme 5 of the European Commission. One of the main goals of TRADEOFF has been to study how the environmental impact of aircraft depends on flight routing and flight altitude. Model experiments using different aircraft

emission scenarios were designed to provide an input for decision making on how to reduce aircraft impact in the future through change of air traffic patterns.

Here we present results from the Oslo CTM-2, a three-dimensional global chemical transport model for the troposphere and the lower stratosphere. The particular strength of this model is the joint application of two comprehensive and well-tested chemistry schemes for the troposphere and the stratosphere, respectively. This, combined with the use of a highly accurate advection scheme and a relatively high vertical resolution in the mid- to high-latitude tropopause region, makes the model suitable for assessing the impact of aircraft emissions. In the following section the model tool is briefly described and evaluated against position data from MOZAIC (Measurement of Ozone and Water Vapor by Airbus In-Service Aircraft). Section 3 deals with the aircraft scenarios used in this study and their implementation in the Oslo CTM-2, while a detailed presentation of results is given in Sect. 4, followed by brief conclusions and future directions in Sect. 5.

2. The Oslo CTM-2

All simulations presented in this paper have been performed with the Oslo CTM-2 model (hereafter 'CTM2'), a global three-dimensional chemical transport model (CTM) for the troposphere and the lower stratosphere, driven by real meteorology from ECMWF (European Centre for Medium range Weather Forecasts). The CTM2 version focusing on tropospheric chemistry has been tested and applied in various papers (e.g. Bregman et al., 2001; Kraabøl et al., 2002; Grini et al., 2002; Isaksen et al., 2005), while the version including both tropospheric and stratospheric chemistry (used in this study) has been used in studies on the impact of water vapor emissions from aircraft (Gauss et al., 2003a) and radiative forcing due to future changes in tropospheric and lower stratospheric ozone (Gauss et al., 2003b). The model is run in 5.6×5.6 degrees horizontal resolution and with 40 sigma-pressure hybrid layers between the surface and 10 hPa. The vertical resolution in the tropopause region varies between about 0.8 km in high latitudes and about 1.2 km in low latitudes. Advective transport

ACPD
5, 12255–12311, 2005

uses the highly-accurate and non-diffusive Second Order Moments scheme (Prather, 1986). Transport through deep convection is parameterized applying the Tiedtke mass flux scheme (Tiedtke, 1989), whereas boundary layer mixing is treated according to the Holtslag K-profile scheme (Holtslag et al., 1990). The calculation of dry deposition follows Wesely (1989), while wet deposition and washout are calculated based on the ECMWF data for convective activity, cloud fraction, and rainout and on the solubility of the species in question. Both large scale and convective washout processes are represented.

For the chemical integrations two comprehensive modules are used, which cover tropospheric and stratospheric chemistry, respectively. The tropospheric chemistry scheme calculates the evolution of 51 species taking into account 86 thermal reactions, 17 photolytic reactions, and 2 heterogeneous reactions. The module includes detailed hydrocarbon chemistry and has been thoroughly tested in the Oslo CTM-1 model (Berntsen and Isaksen, 1997). The stratospheric chemistry solver was developed by Stordal et al. (1985) and Isaksen et al. (1990) and has been extensively used and validated in a stratospheric 3-D CTM (Rummukainen et al., 1999). 158 reactions (104 thermal, 47 photolytic, and 7 heterogeneous) involving a total of 64 species (including 7 families) relevant for the stratosphere are integrated. The model version used in this study applies the scheme of Carslaw et al. (1995) to calculate rate coefficients for heterogeneous reactions occurring on sulfate aerosols and/or polar stratospheric clouds. Sulfate aerosol area densities are retrieved from SAGE satellite measurements for 1999. Both the tropospheric and stratospheric chemistry schemes apply the Quasi Steady State Approximation (QSSA) (Hesstvedt et al., 1978), using gas phase reactions rates from JPL evaluations (DeMore et al., 1997; Sander et al., 2000). Photodissociation rates are calculated on-line once every model hour applying the Fast-J2 method (Bian and Prather, 2002). The tropospheric and stratospheric chemistry modules are, respectively, called below and above the tropopause, which is determined from the NCEP (National Center for Environmental Prediction) reanalysis. It has to be stressed, however, that each transported species is advected throughout the model

ACPD
5, 12255–12311, 2005

domain.

Anthropogenic emissions of source gases (CO, NO_x, Methane, VOC compounds) are the same as in the OxComp model intercomparison study of IPCC-TAR (Prather et al., 2001), based on an extrapolation of the EDGAR 2.0 database (Olivier et al., 1999) to year 2000 conditions. Natural emissions are taken from the Global Emissions Inventory Activity (GEIA, http://geiacenter.org) and Müller (1992). The lightning source is based on zonal-mean data given by Price et al. (1997a, b), scaled to a global output of to 5 Tg(N)/year. Monthly and zonally integrated emission are distributed among all grid cells and meteorological time steps based on local cloud top height and convective activity, following two formulas given by Price et al. (1997a) for continental and marine areas, respectively. The vertical distribution of lighting emissions within a column is computed following Pickering et al. (1998). Aircraft emissions are taken from TRADEOFF inventories as will be described in more detail in Sect. 3. The conversion of emitted NO_x into HNO_3 and other nitrogen reservoir species within the aircraft plume is taken into account following the approach of Kraabøl et al. (2002) using the NILU aircraft plume model (Kraabøl et al., 1999).

The model has been evaluated in a number of earlier publications dealing with different chemical components (e.g. Brunner et al., 2003, 2005; Gauss et al., 2003a; Isaksen et al., 2005; Stevenson et al., 2005). For an additional model evaluation focusing on the UTLS region, where aircraft emissions usually occur, Fig. 1 shows comparisons of CTM2 modeled ozone with MOZAIC aircraft measurements for a selection of flights at different times of the year. The flights have been selected to be representative for the model performance, showing both strengths and weaknesses, and to cover different seasons of the year. Although, due to the rather course spatial and temporal resolutions compared to the dense spacing of MOZAIC measurements, the variability of the MOZAIC measurements on very short time scales is not resolved, the comparison reveals a good overall performance of the model. There is a slight tendency of overestimating ozone in the upper troposphere, which is probably due to too large downward flux of stratospheric ozone and missing loss mechanisms, such as heterogeneous pro-

cessing on cirrus clouds (Solomon et al., 1997; Bregman et al., 2002).

3. Experimental setup

The main characteristics of the 9 model simulations performed for this study are summarized in Table 1. The aircraft emission scenarios were created for TRADEOFF for the year 2000 using the 'FAST' (Future Aviation emissions Scenario Tool) model, developed especially for the purpose of the TRADEOFF studies. FAST calculates global inventories of fuel, NO_x, and km traveled on a global grid, which is variable in horizontal and vertical dimensions as a user-specified input. The calculation methodologies and air traffic movement database were identical to those used in the ANCTAT/EC2 inventory (Gardner et al., 1998). Aircraft were modeled using 16 types and engines, representative of the global fleet. Fuel-flow data for these 16 types were modeled using the same load factor assumptions as in ANCAT/EC2 (i.e. 85%) for a number of mission distances and specified cruise altitudes. The novelty for the TRADEOFF work was the creation of scenarios for the investigation of the impact of polar routes and differing cruise altitudes. The analysis of real mission data from the Eurocontrol and FAA (Federal Aviation Administration) air-space domains, using approximately 53 000 flights, revealed that cruise altitudes correlate with mission distances for the representative aircraft types. In the TRADEOFF scenarios cruise altitudes were prescribed on the basis of this analysis. As the movements database was for 1991/92, a scaling exercise was undertaken to create a year 2000 inventory. The performance of the aircraft fleet was changed according to historical trends in fuel efficiency, which was assumed to be 1.1% improvement per year. The growth in traffic fleet and revenue passenger kilometers between 1992 and 2000 was calculated based on FESG projections (FESG, 1998) for the IS92f scenario (Leggett et al., 1992), as this scenario closely matches year 2000 ICAO (International Civil Aviation Organization) traffic data.

All TRADEOFF scenarios are provided on a $1^{\circ}\times1^{\circ}$ horizontal grid with a vertical interval chosen on the same basis as the real data (i.e. flight level intervals of 2000

ACPD
5, 12255–12311, 2005

feet or 610 m), for 4 different seasons (December to February, March to May, June to August, and September to November). Aircraft NO_x emissions are judged by an emission index, E.I.(NO_x), equal to grams of NO_x (as NO_2) in the exhaust per kilograms of fuel burned. In the TRADEOFF reference case for the year 2000, which is used in model run 'yy', both civil and military aircraft are included with a global annual fuel consumption of about 169 Tg and a global annual nitrogen emission of 0.71 Tg(N)/year, corresponding to an average E.I.(NO_x) of 13.88. The geographical distribution of the annual fuel consumption according to this scenario is plotted in Fig. 2, revealing peak emissions in the North Atlantic Flight Corridor, in North America, Europe and the Far East. Using the NCEP tropopause height in CTM2, about 16% of the global annual NO_x output from aviation is deposited directly into the stratosphere. However, this fraction is strongly dependent on season and latitude due to variations in tropopause height. At low latitudes, where the tropopause is high, aircraft operations occur entirely within the tropopause, while at high latitudes nearly all aircraft emissions are injected into the stratosphere. In mid-latitudes the tropopause height tends to be higher during summer leading to a somewhat smaller fraction of stratospheric emissions than during winter. This in reasonable agreement with what was found by Gettelman et al. (1999), who used both dynamical and thermal tropopause definitions for their analysis of the direct deposition of subsonic aircraft emissions into the stratosphere.

Seven TRADEOFF emission scenarios were designed to examine the tradeoffs in polar routing and changes in flight altitude: One base case and six perturbation cases. These scenarios do not include military aircraft and assume a somewhat higher technology standard in terms of NO_x emission reduction. In the TRADEOFF base case (model run '1') the global annual fuel consumption and nitrogen emission amount to about 152 Tg/year and 0.59 Tg(N)/year, respectively. In two of the perturbation cases a selection of already existing polar routes was significantly enhanced in order to investigate the impact of increased polar routing.

The first one (model run '2a') is normalized with respect to the base case, i.e. the global annual fuel burn and nitrogen emission are identical to those in the base case.

ACPD
5, 12255–12311, 2005

In the second one (model run '2b'), the enhanced polar routing comes in addition to conventional traffic, so that the global annual fuel consumption and nitrogen emission are significantly larger than in the base case. Also, the fraction of emissions occurring in the stratosphere is much larger in the polar route scenarios, reflecting the low tropopause height in high latitudes.

The four remaining scenarios addressed changes in cruising altitude. In order to represent increased and decreased flight altitudes, increments of real flight levels were chosen, i.e. +2000 feet and −6000 feet (+610 m and −1830 m, respectively). The altitude decreases were specified by aircraft type and by mission distance. For the altitude increase some aircraft types for particular mission distances could not perform the flight. Thus, for this latter case, shifts in altitude were made only when feasible.

In the scenarios used for model runs '3a' and '3b', the flight altitude is reduced. Again the first scenario features the same global annual fuel consumption and nitrogen emission as the base case, while in the second one, changes in fuel consumption and nitrogen emissions are taken into account. This approach allows for a separate calculation of the impacts of changed emission altitude and the concomitant change in fuel consumption. As today's cruise altitudes are determined by fuel efficiency considerations, a decrease of 6000 ft in cruise altitudes will lead to an increase in fuel consumption related to increased drag. Accordingly, the total NO_x emission is slightly larger compared to the base case. A considerable reduction is seen in the fraction of emissions released into the stratosphere, which in this case amounts to only 5.8% compared to 16.9% in the base case.

Finally, the emission scenarios applied in model runs '5a' and '5b' address an altitude increase of 2000 ft (610 m). A 2000 feet altitude increase is calculated to lead to a decrease in fuel consumption by 0.5% (owing to reduced drag), but to an increase in NO_x emission of 1.6%. This is due to the fact that those aircraft types that can fly 2000 feet higher have a higher average E.I.(NO_x) at this altitude. In model run '5b' these changes are taken into account, while in model run '5a' the global annual fuel consumption and nitrogen emission are the same as in the base case run. Figure 3

ACPD
5, 12255–12311, 2005

shows the vertical distribution of aircraft NO_x emissions in the base case and the four scenarios dealing with changes in flight altitude.

The meteorology in all model simulations of this study is taken from ECMWF forecast data for the year 2000. First, a multi-year model run is performed without aircraft to provide an initial condition for the 3-dimensional fields of all modeled chemical species. Starting from this initial condition, follow-up runs are integrated for three additional years without aircraft emissions and with aircraft emissions according to the various scenarios described above.

The emissions and tropospheric boundary conditions used are summarized in Table 2. Surface emissions of CH_4 in the year 2000 are mimicked by setting a constant mixing ratio in the lowermost 5 layers of CTM2 (up to about 200 m). 1790 and 1700 ppbv are chosen in the Northern and Southern Hemispheres, respectively. The different perturbation studies considered in this study are summarized in Table 3.

4. Results

4.1. Impact of aircraft emissions in the TRADEOFF reference case

Model simulations '00' and 'yy' are performed to assess the overall effect of NO_x emissions from aircraft, including military aircraft. Figure 4 shows annually averaged zonal-mean changes in NO_y, i.e. total reactive nitrogen, defined as the sum of NO, NO_2, NO_3, N_2O_5, HNO_4, $ClONO_2$, $BrONO_2$, HNO_3, and PAN, and in NO_x, which is the sum of NO and NO_2, due to aircraft emissions in the year 2000. Significant perturbations are confined to the Northern Hemisphere, reflecting the asymmetric distribution of aircraft emissions, with maximum increases amounting to 212 pptv for NO_y and 45 pptv for NO_x. In CTM2 most of the NO_y increase is present as HNO_3, as is apparent from the much smaller NO_x increases. Small decreases of near-surface NO_x are modeled in some areas, probably related to increases in ozone, which converts NO_x into NO_y as found in earlier aircraft studies (Stevenson et al., 1997).

ACPD
5, 12255–12311, 2005

The seasonal variation and locations of the maxima are visualized in Fig. 5. NO_y is significantly enhanced during winter and spring with maximum increases between 250 and 300 pptv in the tropopause region in high Northern latitudes. In CTM2 this corresponds to a relative increase of about 40%. Throughout the year the maximum increase in zonal-mean NO_y is located in mid- to high Northern latitudes between 10 and 12 km. During Northern Hemisphere Summer and in January the maximum increase is located at the North Pole (the northernmost latitude belt of CTM2 is centered at about 86° N). In July and October the increases are somewhat smaller but still significant. The seasonal variation of NO_y perturbations is mainly related to meteorological conditions, in particular the height of the tropopause, which is low in high Northern latitudes during winter allowing aircraft emissions to accumulate more efficiently, and convective transport and washout of NO_y in the troposphere. In particular during July, August, and September convective activity and thus vertical mixing and washout processes in the troposphere are relatively vigorous in CTM2 leading to smaller maximum increases in NO_y at mid latitudes, as was already found in earlier CTM2 studies (Kraabøl et al., 2002). Thus the relatively smaller increase in high latitudes represents the maximum increase in NO_y during this period. Maximum increases in NO_x range from about 40 to almost 70 pptv, depending on season. At night and at large solar zenith angles, the NO_x/NO_y ratio is low, leading to a notable displacement of the maximum NO_x increase towards the equator during Northern Hemisphere winter.

The annual average of zonal-mean ozone and OH changes is shown in Fig. 6. The maximum increase in ozone is located in high Northern latitudes and amounts to 4.3 ppbv, while the maximum increase in OH is seen in mid Northern latitudes reaching 9.4×10^4 molecules cm^{-3}. Above a certain altitude in high southern latitudes ozone is slightly reduced through catalytic NO_x cycles, although this perturbation is not significant. Regarding OH, NO_x emissions lead to a slight enhancement through the reaction of NO and HO_2 and the increase of ozone, which is an OH precursor. Above a certain height in the lower stratosphere, however, decreases in OH are modeled, albeit very small. This is probably connected to the reactions of HNO_3 and HO_2NO_2 with OH,

ACPD
5, 12255–12311, 2005

which gain importance in the stratosphere in mid- to high latitudes in their competition with OH-producing reactions.

The magnitude and latitude of the maximum ozone increase are plotted in Fig. 7. Owing to the close link between sunlight and ozone chemistry, the figure exhibits a strong seasonal variation. Maximum increases are seen during periods coinciding with low solar zenith angles, i.e. late spring and summer. The maximum is located in the northernmost latitude belt during summer, when the sun is present all day, while in winter it is displaced towards the equator, as far as 40° North in the period December to February. The very high latitude of maximum increases during summer is explained by enhanced convective activity during summer, which reduces the ozone increase in mid-latitudes. Excess ozone produced from NO_x emissions in the UTLS is transported into the lower troposphere where the chemical lifetime of ozone is shorter and where it is lost through dry deposition.

The maximum zonal-mean increase in ozone is modeled in June amounting to nearly 8 ppbv, coincident with maximum actinic flux. Relatively small ozone increases between 3 and 4 ppbv are modeled between September and January, resulting from a combination of less sunlight and lower NO_y perturbations due to meteorological conditions.

Table 4 lists changes in total ozone for all perturbations discussed in this paper. For the increase due to aircraft in the TRADEOFF reference case with respect to the 'no aircraft' simulation a global mean increase of about 0.39 DU is modeled, corresponding to an ozone burden increase of 4.24 Tg. For the Northern Hemisphere these values are 0.68 DU and 3.72 Tg, i.e. most of the increase in ozone burden is located in the Northern Hemisphere. Values for changes in the tropospheric ozone column are listed in parenthesis. It is seen that most of the increase in the TRADEOFF reference case occurs in the troposphere. The season-latitude distribution of ozone column change is plotted in Fig. 8. Both the tropospheric and the total (i.e. surface to CTM2 lid) ozone columns are modeled to increase in all seasons and all latitudes. The maximum tropospheric and total column increases are modeled in mid- to high Northern Latitudes

ACPD
5, 12255–12311, 2005

during May and amount to 1.15 DU (2.52%) and 1.34 DU (0.35%), respectively.

The impacts of aircraft NO_x emissions on global tropospheric lifetime of methane are listed in Table 5. The lifetime of methane is expected to decrease due to aircraft-NO_x emissions through the enhancement of OH. Since methane has a relatively long lifetime in the troposphere it is not feasible to calculate changes in methane concentrations directly because of the high CPU demand of CTM2. Rather we estimate changes in methane by changes in its lifetime, which responds instantaneously to changing OH levels. In line with what is done in the IPCC Third Assessment Report (Prather et al., 2001) we apply a chemical feedback factor of 1.4 to account for the longer residence time of a perturbation in methane (Prather, 1994). The resulting radiative forcing is calculated based on the established relation between increases in methane concentration and radiative forcing (Ramaswamy et al., 2001). The lifetime reduction and concomitant radiative forcing calculated for the TRADEOFF reference scenario amount to −0.71% and −6.41 mW/m^2, respectively.

The results of this study can not easily be compared quantitatively with earlier studies, because new aircraft emission scenarios are used here. However, the spatial distribution and seasonal variation of NO_x and ozone changes are similar to what was obtained in earlier studies (Wauben et al., 1997; Stevenson et al., 1997; Berntsen and Isaksen, 1999; Kentarchos and Roelofs, 2002). Köhler et al. (1997) obtained maximum zonal-mean NO_x increases exceeding 50 pptv in both January and July, i.e. somewhat larger than in the present study. This is due to the larger emission source used in their study (i.e. 0.85 Tg(N)/yr), but also to plume chemistry processes reducing both NO_y and NO_x perturbations in our study. Compared to the results of Kentarchos and Roelofs (2002), who used a total aircraft emission source of 0.56 Tg(N)/yr, our maximum ozone increase is further North in July and larger in magnitude, while the perturbations in NO_x are in approximate agreement, especially in January (although it has to be noted that Kentarchos and Roelofs include HNO_4, NO_3 and N_2O_5 in the definition of their NO_x).

ACPD
5, 12255–12311, 2005

4.2. Tradeoffs in enhanced polar routing

Six TRADEOFF scenarios were designed for comparison with the TRADEOFF base case: two scenarios addressing polar routes and four dealing with changes in flight altitudes. The impact of aircraft emissions in the base case simulation ('1') is qualitatively the same as in the reference case ('yy') discussed in Sect. 4.1. Due to the lower emission rate, however, the magnitudes of increase are slightly smaller, which is why the following discussion focuses on the sensitivity of aircraft impact to flight routing rather than the aircraft impact itself.

In recent years polar routes in the Northern Hemisphere have been increasingly used by long range aircraft. For instance, great circle (i.e. shortest) connections between city pairs in Europe and the Western part of North America or between the Far East and the Eastern part of North America go through Arctic regions, and are/will be followed by airlines as closely as possible. Within TRADEOFF the impact of increased polar routing has been studied by enhancing already existing polar routes in the Northern Hemisphere significantly and by analyzing the model response. The strong dependence of chemistry on sunlight combined with the strong seasonality of insolation in high latitudes lead to a large seasonal variability in ozone impact due to aircraft in high latitudes, which is of particular importance when considering increased high latitude routing. Figure 9 shows the change in net chemical production due to polar routing replacing standard routes. In June the impact is clearly revealed, while in December in the absence of sunlight in high Northern latitudes, it is negligible. The slight decrease in mid-latitudes in this perturbation results from a reduction in mid-latitude traffic in this scenario.

Annually averaged zonal-mean changes in ozone are presented in Fig. 10 with respect to the TRADEOFF base case and the 'no aircraft' simulations. In the middle stratosphere signs of ozone depletion due to NO_x emissions are seen, but this effect is negligible in view of the large ambient ozone levels in these altitudes. The decrease of conventional routes manifests itself by the reduced ozone increase in mid- and low

ACPD
5, 12255–12311, 2005

Northern latitudes in the troposphere with respect to the base case. The ozone impact with respect to the 'no aircraft' case reveals appreciable increases in the Arctic.

Figure 11 shows the seasonal variations of the maximum zonal-mean increases in NO_y and ozone, together with the global average increase in total ozone for the polar route scenarios (blue lines) and the other TRADEOFF scenarios to be discussed in Sect. 4.3 (red and green lines), along with the base case perturbations (black line). As shown by the blue lines in the upper panel of the figure, NO_y increases drastically in the polar route scenarios since washout of HNO_3 is less important in high latitudes and absent in the lower stratosphere, in which most of the additional high latitude emissions occur. The latitude of the maximum NO_y increase (not shown) is north of 80° N throughout the year. The maximum increase in zonal-mean ozone (blue line in the middle panel) is strongly influenced by solar radiation, which is a maximum during summer. As the seasonal variation of actinic flux is particularly strong in high latitudes the seasonality of the maximum ozone increase is much more pronounced than in the base case. Indeed, in the normalized polar route scenario during winter, zonal mean increases in ozone are even smaller than in the base case. This is even more pronounced in the total ozone increase shown by the blue lines in the bottom panel of the figure. In the Northern Hemisphere, a replacement of conventional routes by polar routes would reduce the impact on the tropospheric column and increase the stratospheric column on an annual average since more emissions occur in the lower Arctic stratosphere. In the Southern Hemisphere both the increases in tropospheric and stratospheric columns are reduced with respect to the base case, as no high Southern latitude routes are introduced. Judging by the increase in global ozone burden only, a replacement of conventional routes by polar routes would reduce the environmental impact of aircraft with respect to the base case. However, this tradeoff is very small and subject to meteorological conditions such as washout and tropopause height in the Arctic regions, which are subject to interannual variation.

Figure 12 shows the latitude/season distribution of ozone column change due to polar routing replacing standard routes. Due to the poleward shift of aircraft emissions

ACPD
5, 12255–12311, 2005

the increase in both tropospheric and total ozone columns is reduced in low Northern latitudes. Significant increases are confined to the summer season in high Northern latitudes. Regarding the ozone burden, increases in ozone in high latitudes are not compensated by reductions in mid- and low latitudes. Both the increase in ozone burden and the reduction in methane lifetime are thus significantly larger than in the base case.

As listed in Table 5, the reduction in tropospheric methane lifetime is smaller, when polar routes are used instead of conventional routes, as a larger fraction of the aircraft impact occurs in the stratosphere. Accordingly, the magnitude of radiative forcing due to aircraft-induced methane change is almost 20% smaller than in the base case, i.e. $-4.47\,\mathrm{mW/m^2}$ rather than $-5.46\,\mathrm{mW/m^2}$.

4.3. Tradeoffs in changing flight altitude

Since the effects of aircraft NO_x emissions exhibit strong altitudinal dependencies, it has been suggested that the aircraft impact can be reduced by changing flight altitude. Changes in flight altitude will generally lead to modifications in the height profile of ozone change, with the impact getting smaller in certain height regions and larger in others. The key questions to be addressed in this section is to what extent the negative and positive effects cancel each other in terms of total ozone column change, and how the impact on methane lifetime and radiative forcing resulting from methane reductions are modified.

Not surprisingly, lowering the flight altitude reduces aircraft impact at standard flight altitudes, while increasing it at lower altitudes. Figure 13 shows the zonal-mean change in the concentrations of NO_y and NO_x due to a 1830 m reduction in flight altitude taking into account changes in fuel consumption. In low to mid-Northern latitudes, we calculate decreases above 8 to 9 km altitude and increases below, which is a result of lowering the emission source. However, it is important to note that the increase at low altitudes is much smaller in magnitude than the decrease at high altitudes, although the increase in fuel consumption leads to a somewhat larger emission rate at

ACPD
5, 12255–12311, 2005

the new altitude (the Figure shows changes in concentration rather than mixing ratios in order to make this relation clearer). In the case of NO_y, maximum reductions are modeled between 10 and 11 km altitude in Northern mid-latitudes, amounting to -11×10^8 molecules/cm^3, while the maximum increase between 6 and 8 km altitude remains below $+3\times10^8$ molecules/cm^3. For NO_x the corresponding maximum changes are -2.5×10^8 and $+1.1\times10^8$, respectively. This asymmetry is, first and foremost, connected to washout of HNO_3, which is much more efficient at low altitudes, while being virtually absent in the lower stratosphere. The HO_x partitioning (not shown) is shifted towards OH in regions of enhanced NO_x emissions, and towards HO_2 in regions of reduced NO_x emissions. In low latitudes, increases in HO_2 are seen in the troposphere as well. These are regions where HO_x increases as a whole due to the ozone increase. As a result of these changes, the chemical net production, shown in Fig. 14, is enhanced below about 8 km, and reduced above. However, the effect is more pronounced during summer related to larger photochemical activity.

A normalized scenario for the lower flight altitude case was created to estimate the effect from changes in fuel consumption individually. Lowering the cruise altitude will increase air resistance because the air density increases with decreasing altitude in the atmosphere. As a result, fuel consumption and NO_x emissions will increase. Figure 15 shows the separate effect of increasing fuel emission along with the total effect of reducing flight altitude on zonal-mean ozone. Although the magnitude of changes related to fuel consumption is much smaller than the total aircraft effect, it has to be noted that the increase covers all altitudes, i.e. there are no canceling effects between changes of opposite signs at different altitudes. Therefore, in terms of total ozone change, the effect of increased fuel burn is significant compared to the effect from lowering the flight altitude alone.

The total increase in the base case is +0.339 DU (+3.71 Tg). Reducing flight altitude alone ('3a minus 1') leads to a decrease of −0.0266 DU (−0.29 Tg) and increasing fuel use ('3b minus 3a') to +0.0131 DU (+0.14 Tg), so that the total increase due to aircraft in the lower flight altitude scenario ('3b minus 00') amounts to +0.3255 DU (+3.56 Tg).

ACPD
5, 12255–12311, 2005

These findings are in qualitative agreement with the results in a similar study of Grewe et al. (2002b), while the magnitudes of change cannot easily be compared because of the larger total emission from aircraft and the smaller altitude decrease considered in the Grewe et al. study. Also, it has to be noted that the effect on column ozone is strongly dependent on both season and latitude, as reflected by the varying gap between the green dotted and the solid black lines in Fig. 11 (lower panel) and the latitudinal distribution of total ozone change shown in Fig. 16. The reduction in flight altitude leads to decreases in the tropospheric ozone column in low latitudes, which is a clear manifestation of the importance of washout processes. Both in the base case and in the lower-altitude case, virtually all low-latitude aircraft traffic is located in the troposphere, and the lowering of the aircraft emission source results in a larger fraction of emitted nitrogen emissions to be washed out. At mid- to high Northern latitudes an increase in the tropospheric ozone column is modeled. This is due to the enhanced fuel use, and the larger fraction emitted in the troposphere with respect to the base case. However, this increase is overcompensated by a corresponding stratospheric decrease during summer and mid-winter so that the total ozone column change is negative in these seasons, as it is in all seasons at low latitudes. During summer the main reason for this is the high tropopause. A large fraction of aircraft emissions is occurring in the troposphere so that the increase of washout processes and the decrease of ozone lifetime with decreasing altitude are important. On the other hand, during spring and autumn the tropopause tends to be lower and even in the low altitude scenario a very large fraction of aircraft emissions occurs in the stratosphere, where washout does not play a role. The other effect, i.e the decrease in residence times of pollutants in the lower stratosphere with decreasing altitude is not sufficiently important to compensate for the increases in the troposphere. The effect on the total column is thus positive, albeit only slightly.

The next option, an increase in flight altitude by 610 m, is investigated through model runs '5a' and '5b'. Figure 17 shows annually averaged zonal-mean changes in the concentrations of NO_y and NO_x due to a 610 m increase in flight altitude taking into

ACPD

5, 12255–12311, 2005

account changes in fuel consumption and in the total emission of nitrogen. In Northern mid- to high latitudes we calculate increases above 8 to 9 km altitude and decreases below. Again, the effect at high altitudes is larger in magnitude than the effect at low altitudes. For instance, the maximum (high altitude) increase in NO_y amounts to $+4.5\times10^8$ molecules, while the magnitude of the largest reduction is about ten times smaller, -0.43×10^8 molecules/cm^3. This can be in part explained by less efficient washout of excess NO_y at the new (and higher) altitude of emission. Also, the longer effluent lifetime at higher altitudes allows for more pronounced increases and thereby to increased downward flux of NO_y, which partly compensates for the reduced in situ NO_x emissions at lower altitudes. Maximum changes in NO_x and NO_y are displayed in Fig. 11. Slightly larger perturbations are obtained compared to the base case, with the fuel consumption effect being of minor importance.

By and large, increases of the OH/HO_2 ratio (not shown) are seen in regions where the NO_x emission is enhanced, while reductions in NO_x emissions are marked by lower OH and higher HO_2 concentrations. Qualitatively, the effect of higher flight altitude is approximately opposite from what is obtained in the lower-altitude simulations. However, the magnitude of the effect is somewhat smaller, primarily because the change in flight altitude is smaller. The same is true for changes in the chemical net production, which is shown in Fig. 18. The tendency is a reduction below about 8 to 10 km, and an enhancement above, which is most pronounced during summer.

Figure 19 shows the individual effect of changes in fuel consumption and the overall effect of increasing the flight altitude on zonal-mean ozone. The effect of the increased NO_x emission is positive at all altitudes, while the overall effect is slightly negative at low altitudes, positive in the lower stratosphere and again negative in the middle stratosphere, probably due to ozone depletion mechanisms involving NO_x, which is increased at this altitude with respect to simulation '1'. As seen in Table 4 the overall effect on the ozone column due to increased flight altitude is positive both in the stratosphere and in the troposphere. Through the increase in flight altitude the ozone increase is enhanced by 0.0103 DU (0.11 Tg) globally ('5b minus 1'), while the increase

ACPD
5, 12255–12311, 2005

in NO_x emission due to the higher E.I.(NO_x) contributes another 0.0054 DU (0.06 Tg) ('5b minus 5a'), so that the overall effect increase represented by the difference '5b minus 1' amounts to 0.0157 DU (0.17 Tg). Averaged over the Northern Hemisphere the increase equals 0.0207 DU, corresponding to a 0.11 Tg increase of the hemispheric burden.

Figure 20 shows the effect of the increased flight altitude on the ozone column as a function of latitude and season, while the effect on the globally averaged column is depicted by the red lines in Fig. 11 (bottom panel). By and large, the results are opposite to what is obtained for a reduction in flight altitude. In the Southern Hemisphere and in low latitudes of the Northern Hemisphere, there is an increase in both the tropospheric and the stratospheric columns. In mid- to high latitudes the effect on the tropospheric column is negative because of the relatively low tropopause causing a significant reduction in tropospheric emissions in the high-altitude scenario. By contrast, due to the high summer tropopause a large fraction of emission occurs in the troposphere even in the high altitude scenario allowing for increases in the ozone impact related to less efficient washout of pollutants. The effect of enhanced flight altitudes on the total ozone column is positive almost everywhere, except for high Northern latitudes in December. As this exception occurs in the absence of sunlight, it must be related to transport of air that is poorer in ozone compared to the base case.

In Fig. 21 the dependence of changes in tropospheric and stratospheric ozone columns on flight altitude is visualized relative to the changes calculated for the TRADEOFF base case. The perturbations due to a 6000-feet reduction in flight altitude are positive for the tropospheric and negative for the stratospheric ozone columns, which is a consequence of increased tropospheric and reduced stratospheric emissions, respectively. The increase in tropospheric columns is much more pronounced when the increased fuel emission is taken into account. The reduction of the tropospheric methane lifetime and the resultant radiative forcing are more significant due to the lower flight altitude. In simulation '3b' the radiative forcing from methane reductions amounts to $-6.80\,W/m^2$, which is about 25% larger in magnitude than the base case

ACPD
5, 12255–12311, 2005

perturbation (Table 5).

A 2000-feet increase in flight altitude leads to increases in both the tropospheric and the stratospheric ozone column. Increases in the stratosphere are due to increased emissions, while increases in the troposphere are mostly due to increased downward transport of NO_y and resulting increases in tropospheric ozone production. In spite of the slight increase in the tropospheric ozone column, the effect from methane is slightly reduced with respect to the base case simulation, because the methane reduction is slightly smaller. This is related to the vertical distribution of changes in OH (not shown) caused by the higher flight altitude. OH is slightly reduced over a major part of the troposphere leading to an increased lifetime of methane with respect to the base case. This effect is not compensated by the OH increases modeled in the cold upper troposphere where methane oxidation is slower.

5. Conclusions and future directions

In this paper we have presented results from an extensive model study performed for the TRADEOFF project focusing on the environmental impact of aircraft emissions and options to reduce the impact for present conditions (year 2000) and on the impact of aircraft emissions in a future (year 2050) atmosphere. We have used a 3-D chemical transport model including comprehensive chemistry schemes for the troposphere and the stratosphere in order to take into account all chemical processes relevant for the UTLS.

In agreement with earlier studies, significant perturbations in NO_y and NO_x are modeled in the tropopause region of the Northern Hemisphere with a strong zonal variability in the case of NO_x. The resulting maximum perturbations in zonal-mean ozone range between about 3 and 8 ppbv, depending on season. Radiative forcing due to the aircraft-induced reduction in methane amounts to $-6.4\,mW/m^2$ in the reference case for the year 2000. This effect is in the lower end of the range -6 to $-12\,mW/m^2$ reported by the model studies performed in the TRADEOFF project (Isaksen et al., 2003), in

ACPD
5, 12255–12311, 2005

most of which plume processing was less efficient or not modeled.

Emission scenarios regarding enhanced use of polar routes result in significantly enhanced increase in polar stratospheric ozone. However, this increase is confined to the summer season. Judging by ozone changes only, the aircraft impact could thus be reduced by enhanced use high latitude routes during winter.

Another investigation in this study has investigated the impact of changes in flight altitude based on realistic aircraft emission scenarios. Changes in flight altitude modify the vertical profile of ozone changes. In terms of annually averaged total ozone column change, an increase in flight altitude leads to a larger impact, while a reduction in flight altitude leads to a smaller impact than in the scenario assuming standard flight altitudes. However, these effects are highly dependent on season, latitude, and local meteorological conditions. In mid- to high Northern latitudes during summer, lowering the flight altitude significantly reduces the aircraft impact on ozone, while in spring and autumn, larger ozone column increases are modeled. Increasing the flight altitude is calculated to result in larger total ozone increases in all seasons and latitudes, with the exception of high Northern latitudes in late autumn in the absence of sunlight.

Aircraft-induced changes in ozone and modifications in the height profile of ozone change will alter radiative forcing exerted by ozone. Radiative forcing calculations are being performed based on the ozone perturbations discussed in this paper (G. Myhre, University of Oslo, personal communication) and will be published in the near future (Stordal et al., 2005[1]). In addition, it is planned to run the CTM on a higher horizontal resolution with meteorology from other years than 2000, to include PAN and acetone chemistry explicitly in the stratospheric chemistry package, and chlorine chemistry in the tropospheric module.

In terms of the potential climate impact from aircraft, it has to be noted that this study only deals with changes in ozone and methane. In order to make practical suggestions on how to reduce aircraft impact by changes in flight altitude and routing, these results

[1]Stordal, F., Myhre, G., Gauss, M., et al.: Radiative forcing from ozone and methane due to air traffic: TRADEOFFs in alternative routing, in preparation, 2005.

have to be considered in connection with other aspects of aircraft impact on the environment. For example, changes in flight routing will, in general, lead to changes in fuel consumption and thus in emissions of CO_2, a major greenhouse gas. Contrails and cirrus clouds constitute another important climate impact from aircraft (e.g. Marquart et al., 2003; Isaksen et al., 2003). Their formation is largely controlled by the ambient meteorological conditions including pressure and humidity and therefore is strongly dependent on flight altitude and latitude. The resulting radiative forcing depends on their optical properties, solar zenith angle, and natural cloud cover, all of which need to be modeled accurately.

Following an integrated analysis of all aspects of aircraft impact for different atmospheric conditions and options for flight routing, suggestions on how to reduce the environmental impact have to be examined together with safety considerations and air traffic restrictions before decisions can be taken. The present study has thus to be viewed as one important input to the overall assessment of the environmental impact of civil aviation.

Acknowledgements. This study is a part of the TRADEOFF project, which was supported by the European Commission through the Fifth Framework Programme. The model development was mainly funded by the Research Council of Norway through the COZUV project.

The model validation, part of which is presented in this study, has greatly profited from the MOZAIC Programme (http://www.aero.obs-mip.fr/mozaic/). NCEP Reanalysis data for tropopause pressure was provided by the NOAA-CIRES Climate Diagnostics Center, Boulder, Colorado, USA, from their Web site at http://www.cdc.noaa.gov/.

References

Airbus, S. A. S.: Global Market Forecast, 31707 BLAGNAC CEDEX, France, Reference CB 390.0008/02, 2002.

Berntsen, T. and Isaksen, I. S. A.: A global 3-D chemical transport model for the troposphere, 1, Model description and CO and Ozone results, J. Geophys. Res., 102(D23), 21 239–21 280, 1997.

Berntsen, T. K. and Isaksen, I. S. A.: Effects of lightning and convection on changes in upper tropospheric ozone due to aircraft, Tellus, 51B, 766–788, 1999.

Bian, H. S. and Prather, M. J.: Fast-J2: Accurate simulation of stratospheric photolysis in global chemical models, J. Atmos. Chem., 41 (3), 281–296, 2002.

Brasseur, G., Cox, R., Hauglustaine, D., Isaksen, I. S. A., Lelieveld, J., Lister, D., Sausen, R., Schumann, U., Wahner, A., and Wiesen, P.: European scientific assessment of the atmospheric effect of aircraft emissions, Atmos. Environ., 32, 2329–2418, 1998.

Bregman, A., Krol, M. C., Teyssedre, H., Norton, W. A., Iwi, A., Chipperfield, M. Pitari, G., Sundet, J. K., and Lelieveld, J.: Chemistry-transport model comparison with ozone observation in the midlatitude lowermost stratosphere, J. Geophys. Res., 106(D15), 17 479–17 489, 2001.

Bregman, B., Wang, P. H., and Lelieveld, J.: Chemical ozone loss in the tropopause region on subvisible ice clouds, calculated with a chemistry-transport model, J. Geophys. Res., 107(D3), doi:10.1029/2001JD000761, 2002.

Brühl, C., Pöschl, U., Crutzen, P., and Steil, B.: Acetone and PAN in the upper troposphere: Impact on ozone production from aircraft emissions, Atmos. Environ., 34, 3931–3938, 2000.

Brunner, D., Staehelin, J., Rogers, H. L., Köhler, M. O., Pyle, J. A., Hauglustaine, D. A., Jourdain, L., Berntsen, T. K., Gauss, M., Isaksen, I. S. A., Meijer, E., van Velthoven, P., Pitari, G., Mancini, E., Grewe, V., and Sausen, R.: An evaluation of the performance of chemistry transport models by comparison with research aircraft observations. Part 1: Concepts and overall model performance, Atmos. Chem. Phys., 3, 1609–1631, 2003, SRef-ID: 1680-7324/acp/2003-3-1609.

Brunner, D., Staehelin, J., Rogers, H. L., Köhler, M. O., Pyle, J. A., Hauglustaine, D. A., Jourdain, L., Berntsen, T. K., Gauss, M., Isaksen, I. S. A., Meijer, E., van Velthoven, P., Pitari, G., Mancini, E., Grewe, V., and Sausen, R.: An evaluation of the performance of chemistry transport models – Part 2: Detailed comparison with two selected campaigns, Atmos. Chem. Phys., 5, 107–129, 2005, SRef-ID: 1680-7324/acp/2005-5-107.

Carslaw, K., Luo, B., and Peter, T.: An analytic expression for the composition of aqueous HNO_3+H_2SO_4 stratospheric aerosols including gas phase removal of HNO_3, Geophys. Res. Lett., 22(14), 1877–1880, 1995.

Crutzen, P. J.: The influence of nitrogen oxides on atmospheric ozone content, Q. J. R. Meteorol. Soc., 96, 320–325, 1970.

Dameris, M., Grewe, V., Köhler, I., Sausen, P., Bruehl, C., Grooss, J., and Steil, B.: Impact of aircraft NO_x emissions on tropospheric and stratospheric ozone, Part II, 3D model results, Atmos. Environ., 32, 3185–3199, 1998.

DeMore, W. G., Sander, S. P., Golden, D. M., Hampson, R. F., Kurylo, M. J., Howard, C. J., Ravishankara, A. R., Kolb, C. E., and Molina, M. J.: Chemical Kinetics and Photochemical Data for Use in Stratospheric Modeling, Evaluation No. 12, JPL Publication 97-4, Jet Propulsion Laboratory, Pasadena, CA, 1997.

Fabian, P. and Kärcher, B.: The impact of aviation upon the atmosphere, Phys. Chem. Earth, 22, 503–598, 1997.

FESG: Report of the Forecasting and Economic Support Group to CAEP/4. International Civil Aviation Organization Committee on Aviation Environmental Protection, Montreal Canada, 6–8 April 1998, 132 pp, 1998.

Gardner, R. M., Adams, J. K., Cook, T., Lason, L. G., Falk, R. S., Fleuti, E., Förtsch, W., Lecht, M., Lee, D. S., Leech, M. V., Lister, D. H., Massé, B., Morris, K., Newton, P. J., Owen, A., Parker, E., Schmitt, A., ten Have, H., and Vandenbergh, C.: ANCAT/EC2 Global Aircraft Emission Inventories for 1991/92 and 2015, Report by the ECAC/ANCAT and EC working group, EUR-18179, 1998.

Gauss, M., Isaksen, I. S. A., Wong, S., and Wang, W.-C.: Impact of H_2O emissions from cryoplanes and kerosene aircraft on the atmosphere, J. Geophys. Res., 108(D10), 4304, doi:10.1029/2002JD002623, 2003a.

Gauss, M., Myhre, G., Pitari, G., Prather, M. J., Isaksen, I. S. A., Berntsen, T. K., Brasseur, G. P., Dentener, F. J., Derwent, R. G., Hauglustaine, D. A., Horowitz, L. W., Jacob, D. J., Johnson, M., Law, K. S., Mickley, L. J., Müller, J.-F., Plantevin, P.-H., Pyle, J. A., Rogers, H. L., Stevenson, D. S., Sundet, J. K., van Weele, M., and Wild, O.: Radiative forcing in the 21st century due to ozone changes in the troposphere and the lower stratosphere, J. Geophys. Res., 108(D9), doi:10.1029/2002JD002624, 2003b.

Gettelman, A. and Baughcum, S.: Direct deposition of subsonic aircraft emissions into the stratosphere, J. Geophys. Res., 104(D7), 8317–8327, 1999.

Grewe, V., Dameris, M., Fichter, C., and Sausen, R.: Impact of aircraft NO_x emissions. Part 1: Interactively coupled climate-chemistry simulations and sensitivities to climate-chemistry feedback, lightning and model resolution, Meteorol. Z., 11 (3), 177–186, 2002a.

Grewe, V., Dameris, M., Fichter, C., and Lee, D. S.: Impact of aircraft NO_x emissions. Part 2: Effects of lowering the flight altitude, Meteorol. Z., 11 (3), 197–205, 2002b.

Grini, A., Myhre, G., Sundet, J. K., and Isaksen, I. S. A.: Modeling the annual cycle of sea salt in the global 3-D model Oslo CTM-2, concentration, fluxes and radiative impact, J. Clim., 15, 1717–1730, 2002.

Hansen, J., Sato, M., and Ruedy, R.: Radiative forcing and climate response, J. Geophys. Res., 102(D6), 6831–6864, 1997.

Hesstvedt, E., Hov, O., and Isaksen, I. S. A.: Quasi steady-state approximation in air pollution modelling: Comparison of two numerical schemes for oxidant prediction, Int. J. Chem. Kinetics, X, 971–994, 1978.

Hidalgo, H. and Crutzen, P. J.: The tropospheric and stratospheric composition perturbed by NO_x emissions of high-altitude aircraft, J. Geophys. Res., 82, 5833–5866, 1977.

Holtslag, A. A. M., DrBruijn, E. I. F., and Pan, H.-L.: A High resolution air mass transformation model for short-range weather forecasting, Mon. Wea. Rev., 118, 1561–1575, 1990.

Isaksen, I. S. A., Rognerud, B., Stordal, F., Coffey, M. T., and Mankin, W. G.: Studies of Arctic stratospheric ozone in a 2-d model including some effects of zonal asymmetries, Geophys. Res. Lett., 17, 557–560, 1990.

Isaksen, I. S. A., Berntsen, T. K., and Wang, W.-C.: NO_x Emissions from Aircraft: Its Impact on the Global Distribution of CH_4 and O_3 and on Radiative Forcing, Terrestrial, Atmos. Ocean. Sci., 12, 1, 63–78, 2001.

Isaksen, I. S. A., Sausen, R., Pyle, J. A., et al.: The EU project TRADEOFF – Aircraft emissions: Contributions of various climate compounds to changes in composition and radiative forcing – tradeoff to reduce atmospheric impact, Project Final report, Contract No. EVK2-CT-1999-0030 (available from the Department of Geosciences, University of Oslo, Oslo, Norway), 158 pp, 2003.

Isaksen, I. S. A., Zerefos, C., Kourtidis, K., Meleti, C., Dalsoren, S. B., Sundet, J. K., Grini, A., Zanis, P., and Balis, D.: Tropospheric ozone changes at unpolluted and semipolluted regions induced by stratospheric ozone changes, J. Geophys. Res., 110(D2), doi:10.1029/2004JD004618, 2005.

Jaeglé, L., Jacob, D. J., Brune, W. H., Tan, D., Faloona, I. C., Weinheimer, A. J., Ridely, B. A., Campos, T. L., and Sachse, G. W.: Sources of HO_x and ozone production in the upper troposphere over the United States, Geophys. Res. Lett., 25(10), 1709–1712, 1998.

Jaeglé, L., Jacob, D. J., Brune, W. H., Faloona, I. C., Tan, D., Kondo, Y., Sachse, G. W., Anderson, B., Gregory, G. L., Vay, S., Singh, H. B., Blake, D. R., and Shetter, R.: Ozone production in the upper troposphere and the influence of aircraft during SONEX: Approach

of NO_x-saturated conditions, Geophys. Res. Lett., 26(20), 3081–3084, 1999.
Johnson, C. E., Henshaw, J., and McInnes, G.: Impact of aircraft and surface emissions of nitrogen oxides on tropospheric ozone and global warming, Nature, 355, 69–71, 1992.
Johnston, H. S.: Reduction of stratospheric ozone by nitrogen oxide catalysts from supersonic transport exhaust, Science, 173, 517–522, 1971.
Kentarchos, A. S. and Roelofs, G. J.: Impact of aircraft NO_x emissions on tropospheric ozone calculated with a chemistry-general circulation model: Sensitivity to higher hydrocarbon chemistry, J. Geophys. Res., 107(D13), doi:10.1029/2001JD000828, 2002.
Köhler, I., Sausen, R., and Reinberger, R.: Contribution of aircraft emissions to the atmospheric NO_x content, Atmos. Environ., 31, 1801–1818, 1997.
Kraabøl, A. G., Stordal, F., Konopka, P., and Knudsen, S.: The NILU aircraft plume model: A technical description, NILU Tech. Rep., TR 4/99, Norwegian Institute for Air Research, Norway, 1999.
Kraabøl, A. G., Berntsen, T. K., Sundet, J. K., and Stordal, F.: Impacts of NO_x emissions from subsonic aircraft in a global three dimensional chemistry transport model including plume processes J. Geophys. Res., 107(D22), doi:10.1029/2001JD001019, 2002.
Lacis, A. A., Wuebbles, D. J., and Logan, J. A.: Radiative forcing by changes in the vertical distribution of ozone, J. Geophys. Res., 95, 9971–9981, 1990.
Lee, D. S., Köhler, I., Grobler, E., Rohrer, F., Sausen, R., Gallardo-Klenner, L., Olivier, J. J. G., and Dentener, F. D.: Estimations of global NO_x emissions and their uncertainties, Atmos. Environ., 31, 1735–1749, 1997.
Leggett, J., Pepper, W. J., and Swart, R. J.: Emissions scenarios for the IPCC: an update, in: Climate Change 1992: The Supplementary Report to the IPCC Scientific Assessment, prepared by: IPCC Working Group I (edited by: Houghton, J. T., Callander, B. A., and Varney, S. K.) and WMO/UNEP, Cambridge University Press, Cambridge, United Kingdom, and New York, NY, USA, 1992.
Marquart S., Ponater, M., Mager, F., and Sausen, R.: Future development of contrail cover, optical depth, and radiative forcing: Impacts of increasing air traffic and climate change, J. Clim., 16 (17), 2890–2904, 2003.
Müller, J. F.: Geographical distribution and seasonal variation of surface emissions and deposition velocities of atmospheric trace gases, J. Geophys. Res., 97, 3787–3804, 1992.
Olivier, J. G. J., Bouwman, A. F., Berdowski, J. J. M., Veldt, C., Bloos, J. P. J., Visschedijk, A. J. H., van der Maas, C. W. M., and Zasndveld, P. Y. J.: Sectoral emission inventories of

greenhouse gases for 1990 on a per country basis as well as on 1×1, Envir. Sci. Policy, 2, 241–263, 1999.
Penner, J. E., Lister, D. H., Griggs, D. J., Dokken, D. J., and McFarland, M.: Aviation and the Global Atmosphere. A special report of IPCC Working Groups I and III, 373 pp., Cambridge Univ. Press, Cambridge, UK, 1999.
Pickering, K. E., Wang, Y. S., Tao, W. K., Price, C., and Müller, J. F.: Vertical distributions of lightning NO_x for use in regional and global chemical transport models, J. Geophys. Res., 103(D23), 31 203–31 216, 1998.
Prather, M. J.: Numerical advection by conservation of second-order moments, J. Geophys. Res., 91, 6671–6681, 1986.
Prather, M. J.: Lifetimes and eigenstates in atmospheric chemistry, Geophys. Res. Lett., 21(9), 801–804, 1994.
Prather, M., Ehhalt, D., Dentener, F., Derwent, R., Dlugokencky, E., Holland, E., Isaksen, I., Katima, J., Kirchhoff, V., Matson, P., Midgley, P., and Wang, M.: Atmospheric Chemistry and Greenhouse Gases, in: Climate Change 2001: The Scientific Basis, Contribution of Working Group I to the Third Assessment Report of the Intergovernmental Panel on Climate Change (IPCC), edited by: Houghton, J. T., Ding, Y., Griggs, D. J., Noguer, M., van der Linden, P. J., Dai, X., Maskell, K., and Johnson, C. A., Cambridge University Press, Cambridge, United Kingdom and New York, NY, USA, 881 pp, 2001.
Price, C., Penner, J., and Prather, M.: NO_x from lightning 1. Global distribution based on lightning physics, J. Geophys. Res., 102(D5), 5929–5942, 1997a.
Price, C., Penner, J., and Prather, M.: NO_x from lightning 2. Constraints from the global atmospheric circuit, J. Geophys. Res., 102(D5), 5943–5952, 1997b.
Ramaswamy, V., Boucher, O., Haigh, J., Hauglustaine, D., Haywood, J., Myhre, G., Nakajima, T., Shi, G. Y., and Solomon, S.: Radiative Forcing of Climate Change, in: Climate Change 2001: The Scientific Basis. Contribution of Working Group I to the Third Assessment Report of the Intergovernmental Panel on Climate Change (IPCC), edited by: Houghton, J. T., Ding, Y., Griggs, D. J., Noguer, M., van der Linden, P. J., Dai, X., Maskell, K., and Johnson, C. A., Cambridge University Press, Cambridge, United Kingdom and New York, NY, USA, 881 pp, 2001.
Rummukainen, M., Isaksen, I. S. A., Rognerud, B., and Stordal, F.: A global model tool for three-dimensional multiyear stratospheric chemistry simulations: Model description and first results, J. Geophys. Res., 104(D21), 26 437–26 456, 1999.

Sander, S. P., Friedl, R. R., DeMore, W. B., Golden, D. M., Kurylo, M. J., Hampson, R. F., Huie, R. E., Moortgat, G. K., Ravishankara, A. R., Kolb, C. E., and Molina, M. J.: Chemical Kinetics and Photochemical Data for Use in Stratospheric Modeling, Evaluation No. 13, JPL Publication 00-3, Jet Propulsion Laboratory, Pasadena, CA, 2000.

Schumann, U.: The impact of nitrogen oxides emissions from aircraft upon the atmosphere at flight altitudes – Results from the AERONOX project, Atmos. Environ., 31, 1723–1733, 1997.

Schumann, U., Schlager, H., Arnold, F., Ovarlez, J., Kelder, H., Hov, Ø., Hayman, G., Isaksen, I., Staehelin, J., and Whitefield, P.: Pollution from aircraft emissions in the North Atlantic Flight Corridor: Overview on the POLINAT projects, J. Geophys. Res., 105(D3), 3605–3631, 2000.

Solomon, S., Borrmann, S., Garcia, R. R., Portmann, R., Thomason, L., Poole, L. R., Winker, D., and McCormick, M. P.: Heterogeneous chlorine chemistry in the tropopause region, J. Geophys. Res., 102(D17), 21 411–21 429, 1997.

Stevenson, D., Collins, W., Johnson, C., and Derwent, R.: The impact of aircraft nitrogen oxide emissions on tropospheric ozone studied with a 3D Lagrangian model including fully diurnal chemistry, Atmos. Environ., 31, 1837–1850, 1997.

Stevenson, D. S., Dentener, F. J., Schultz, M. G., Ellingsen, K., van Noije, T. P. C., Wild, O., Zeng, G., Amann, M., Atherton, C. S., Bell, N., Bergmann, D. J., Bey, I., Butler, T., Cofala, J., Collins, W. J., Derwent, R. G., Doherty, R. M., Drevet, J., Eskes, H. J., Fiore, A. M., Gauss, M., Hauglustaine, D. A., Horowitz, L. W., Isaksen, I. S. A., Krol, M. C., Lamarque, J.-F., Lawrence, M. G., Montanaro, V., Müller, J.-F., Pitari, G., Prather, M. J., Pyle, J. A., Rast, S., Rodriguez, J. M., Sanderson, M. G., Savage, N. H., Shindell, D. T., Strahan, S. E., Sudo, K., and Szopa, S.: Multi-model ensemble simulations of present-day and near-future tropospheric ozone, J. Geophys. Res., in press, 2005.

Stordal, F., Isaksen, I. S. A., and Horntvedt, K.: A diabatic circulation two-dimensional model with photochemistry: Simulations of ozone and long-lived tracers with surface sources, J. Geophys. Res., 90, 5757–5776, 1985.

Tiedtke, M.: A Comprehensive Mass Flux Scheme for Cumulus Parameterisation on Large Scale Models, Mon. Weather Rev., 117, 1779–1800, 1989.

van Velthoven, P. F. J., Wauben, W. M. F., Kelder, H., Köhler, I., Sausen, R., and Rohrer, F.: The passive transport of NO_x emissions from aircraft studied with a hierarchy of models, Atmos. Environ., 31, 1783–1799, 1997.

Wang, W.-C. and Sze, N. D.: Coupled effects of atmospheric N_2O and O_3 on the Earth's climate, Nature, 286, 589–590, 1980.
Wauben, W., van Velthoven, P., and Kelder, H.: A 3D chemistry transport model study of the changes in atmospheric ozone due to aircraft NO_x emissions, Atmos. Environ., 31, 1819–1836, 1997.
Wesely, M. L.: Parameterization of surface resistances to gaseous dry deposition in regional-scale numerical models, Atmos. Environ., 23, 1293–1304, 1989.
World Meteorological Organization (WMO): Scientific assessment of ozone depletion: 1998, Global ozone research and monitoring project – Report 44, Geneva, Switzerland, 732 pp, 1999.

ACPD
5, 12255–12311, 2005

Table 1. Summary of the model simulations and TRADEOFF aircraft emission scenarios.

Model run	Aircraft emission scenario used	Fuel burn Tg/year	Total nitrogen emission[1)] Tg(N)/year	E.I.(NO_x) fleet average[2)]
00	no aircraft	–	–	–
yy	reference case	169.01	0.7138 (15.63%)	13.88
1	base case	151.95	0.5942 (16.92%)	12.85
2a	additional polar routes, normalized[3)]	151.95	0.5942 (34.12%)	12.85
2b	additional polar routes, changed fuel burn[3)]	204.01	0.8548 (34.08%)	13.77
3a	lower cruise altitude (−6000 ft), normalized[3)]	151.95	0.5942 (5.83%)	12.85
3b	lower cruise altitude (−6000 ft), changed fuel burn[3)]	160.82	0.6204 (5.83%)	12.68
5a	higher cruise altitude (+2000 ft), normalized[3)]	151.95	0.5942 (20.03%)	12.85
5b	higher cruise altitude (+2000 ft), changed fuel burn[3)]	151.16	0.6040 (20.03%)	13.13

[1)] The fraction of aircraft emissions occurring in the stratosphere is given in parenthesis (see Sect. 4.2).
[2)] The NO_x emission index, E.I.(NO_x), is defined as grams of NO_x (as NO_2) emitted per kg of burnt fuel.
[3)] Changes in flight routing will in general imply changes in fuel burn. In the 'changed fuel burn' cases this effect is taken into account, while the 'Normalized' scenarios use the same total fuel burn as in the base case.

ACPD
5, 12255–12311, 2005

Table 2. Emissions and boundary conditions used in the model simulations.

Species	Mixing ratio/emission
CH_4	1745 ppbv
CO	547 Tg(CO)/year
VOC	133 Tg(C)/year
NO_x – Biofuel	2.41 Tg(N)/year
NO_x – Fossil Fuel	25.55 Tg(N)/year
NO_x – Industry	2.01 Tg(N)/year
NO_x – Biomass burning	5.84 Tg(N)/year
NO_x – Soils	8.01 Tg(N)/year
NO_x – Lightning	5.00 Tg(N)/year
NO_x – Aircraft	0.59–0.71 Tg(N)/year (depending on scenario)
N_2O	318 ppbv
Cly (ETCL)[1)]	3.54 ppbv
Bry (ETBL)[2)]	16.34 pptv

[1)] Equivalent Tropospheric Chlorine Loading (WMO, 1999)
[2)] Equivalent Tropospheric Bromine Loading (WMO, 1999)

ACPD
5, 12255–12311, 2005

Table 3. Summary of the various effects discussed in this paper. Perturbations with respect to the 'no aircraft' case are not listed except for the reference case.

Perturbation	Effect quantified
yy minus 00	best estimate of aircraft impact in 2000
2a minus 1	impact of enhanced polar routing replacing standard routes
2b minus 1	impact of additional polar routes
3a minus 1	impact of lower cruise altitude
3b minus 3a	impact of associated change in fuel burn
3b minus 1	impact of lower cruise altitude and associated change in fuel burn
5a minus 1	impact of higher cruise altitude
5b minus 5a	impact of associated change in fuel burn
5b minus 1	impact of higher cruise altitude and associated change in fuel burn

ACPD

5, 12255–12311, 2005

Table 4. Changes in the total ozone column and, in parenthesis, the tropospheric ozone column, averaged over the globe and over the Northern Hemisphere in the various model simulations discussed in this and the following sections (units: DU). In order to obtain ozone burden change in Tg, global averages and Northern Hemisphere averages (in DU) have to be multiplied by 10.93 Tg/DU and 5.47 Tg/DU, respectively.

Model run	Global average:		Northern Hemisphere average:	
	δ total ozone with respect to '00' (DU)	δ total ozone (DU) with respect to '1'	δ total ozone (DU) with respect to '00'	δ total ozone (DU) with respect to '1'
yy	+0.3876 (+0.3321)		+0.6807 (+0.5796)	
1	+0.3390 (+0.2889)		+0.5928 (+0.5017)	
2a	+0.3314 (+0.2701)	−0.0076 (−0.0188)	+0.5942 (+0.4825)	+0.0014 (−0.0192)
2b	+0.4518 (+0.3715)	+0.1128 (+0.0826)	+0.8059 (+0.6605)	+0.2131 (+0.1589)
3a	+0.3124 (+0.2867)	−0.0266 (−0.0022)	+0.5512 (+0.5028)	−0.0416 (+0.0011)
3b	+0.3255 (+0.2987)	−0.0135 (+0.0098)	+0.5741 (+0.5237)	−0.0187 (+0.0221)
5a	+0.3493 (+0.2923)	+0.0103 (+0.0034)	+0.6042 (+0.5020)	+0.0114 (+0.0003)
5b	+0.3547 (+0.2968)	+0.0157 (+0.0079)	+0.6135 (+0.5096)	+0.0207 (+0.0080)

ACPD
5, 12255–12311, 2005

Table 5. Change in chemical tropospheric lifetime of CH_4 due to aircraft-induced perturbations. Resulting radiative forcing is listed for the perturbations with respect to the 'no aircraft' case.

Perturbation	$\delta\tau CH_4$ in percent and percent per Tg(N) emitted	Radiative forcing (mW/m^2)
yy–00	−0.7068% (−0.99%/Tg(N))	−6.41
1–00	−0.6030% (−1.01%/Tg(N))	−5.46
2a–00	−0.4931% (−0.83%/Tg(N))	−4.47
2a–1	+0.1106%	
2b–00	−0.6908% (−0.81%/Tg(N))	−6.26
2b–1	−0.0883%	
3a–00	−0.7203% (−1.21%/Tg(N))	−6.53
3a–1	−0.1180%	
3b–00	−0.7502% (−1.21%/Tg(N))	−6.80
3b–1	−0.1480%	
3b–3a	−0.0301%	
5a–00	−0.5903% (−0.99%/Tg(N))	−5.35
5a–1	+0.0128%	
5b–00	−0.5996% (−0.99%/Tg(N))	−5.43
5b–1	+0.0035%	
5b–5a	−0.0039%	

ACPD

5, 12255–12311, 2005

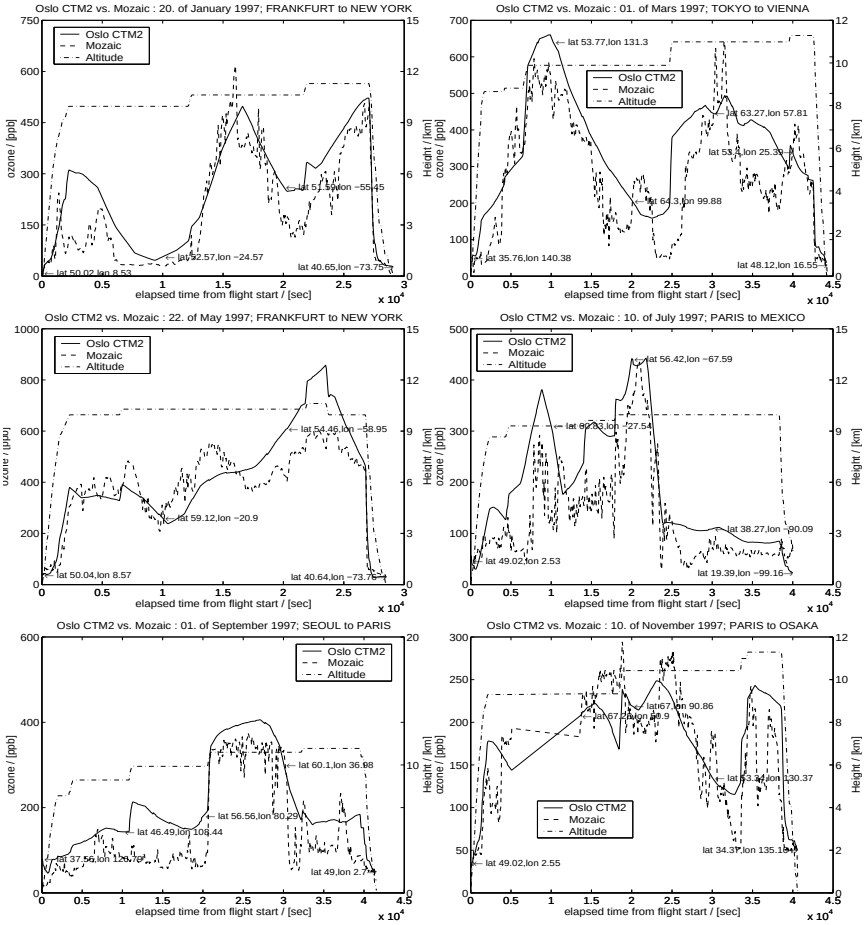

Fig. 1. Comparisons of CTM2 data (solid lines) with simultaneous aircraft measurements (MOZAIC, dashed lines) for ozone mixing ratio (ppbv). Dashed-dotted lines depict the altitude of the measurements. The geographical location of the measurement is indicated every hour and prior to landing.

ACPD
5, 12255–12311, 2005

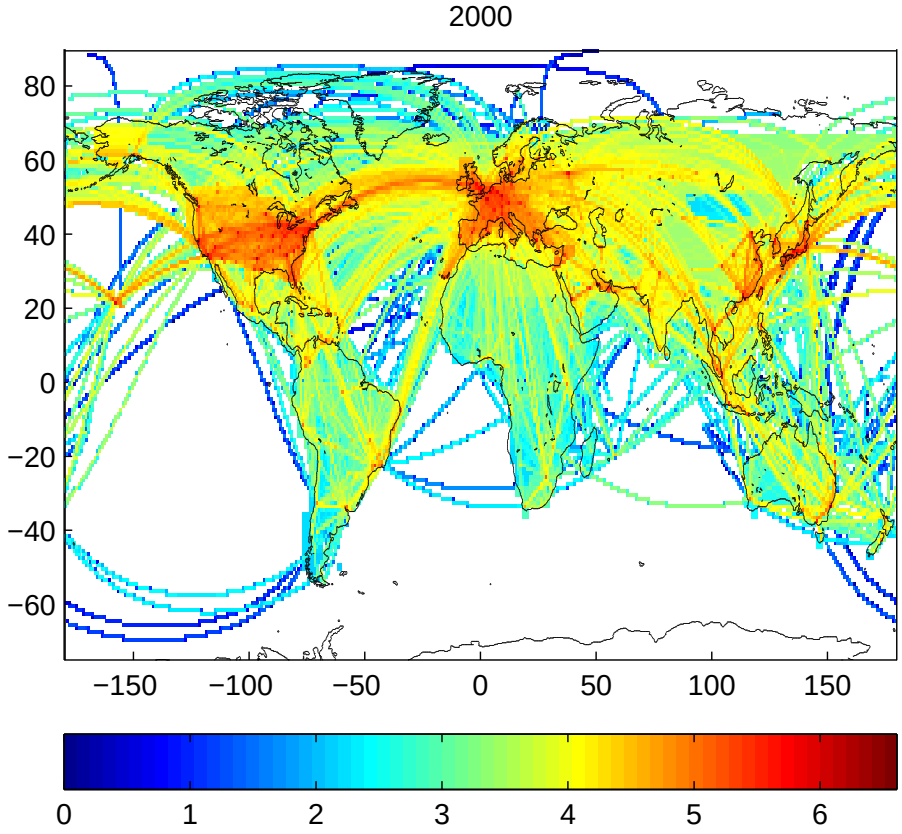

Fig. 2. Geographical distribution of aviation fuel burn in the TRADEOFF reference case (year 2000), vertically integrated for each 1°×1° column. Unit: $\log_{10}$ [kg(fuel)/(day*1°×1°column)].

ACPD

5, 12255–12311, 2005

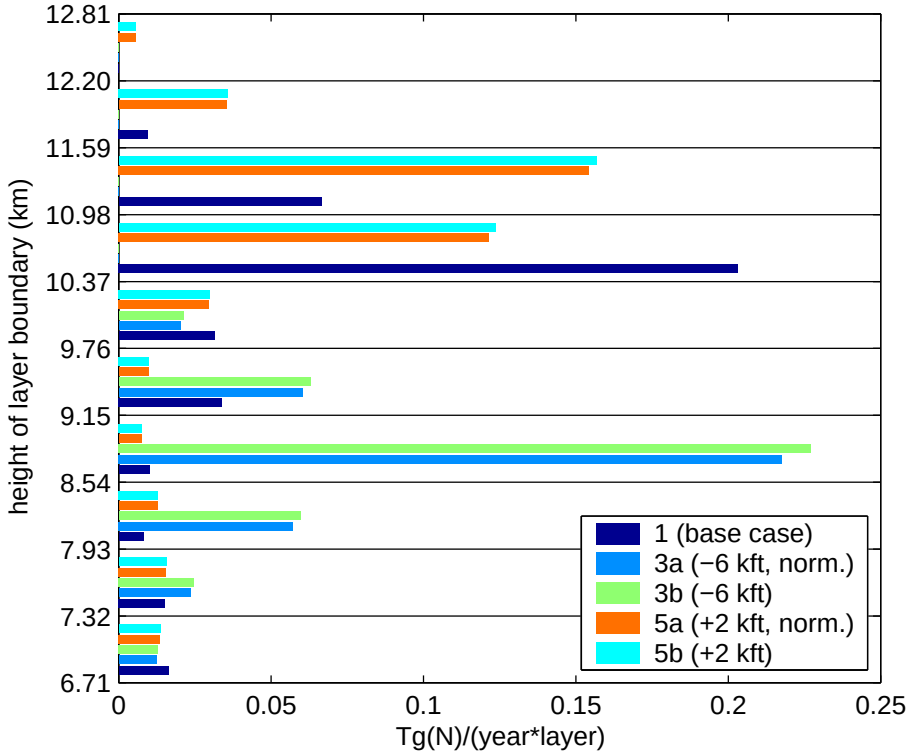

Fig. 3. Total annual NO_x injection into flight levels between 6710 m and 12 810 m according to the TRADEOFF scenarios used in model runs '1' (base case), '3a' (−6000 feet, normalized), '3b' (−6000 feet), '5a' (+2000 feet, normalized), and '5b' (+2000 feet), plotted as Tg(N)/(year*610 m−layer). Thin horizontal lines depict flight level boundaries. Above 12 810 m there are no aircraft emissions in the TRADEOFF scenarios.

ACPD
5, 12255–12311, 2005

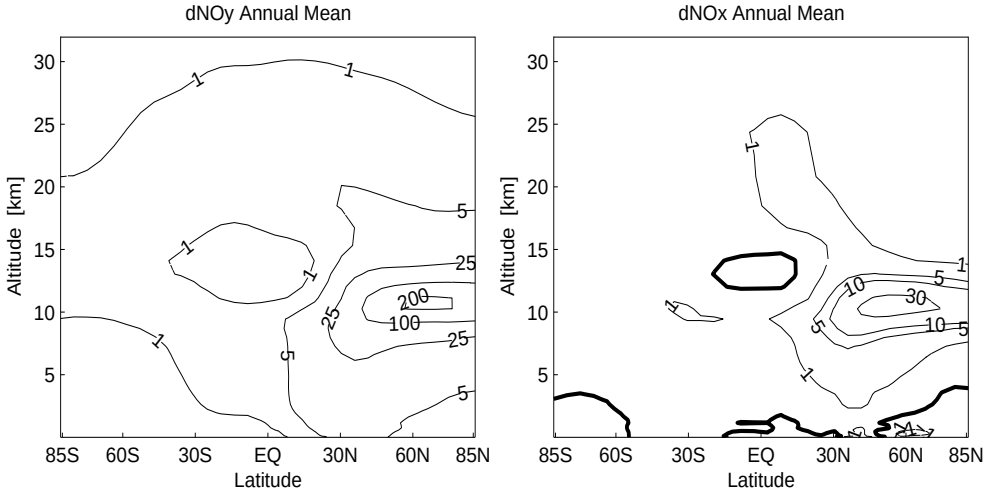

Fig. 4. Annually averaged changes in zonal-mean NO_y (left) and NO_x (right) due to aircraft emissions in the TRADEOFF reference case, i.e. 'yy–00' (units: pptv). Contours at −1, 0, 1, 5, 25, 100, 200 for NO_y, and −1, 0, 1, 5, 10, 30 for NO_x.

ACPD
5, 12255–12311, 2005

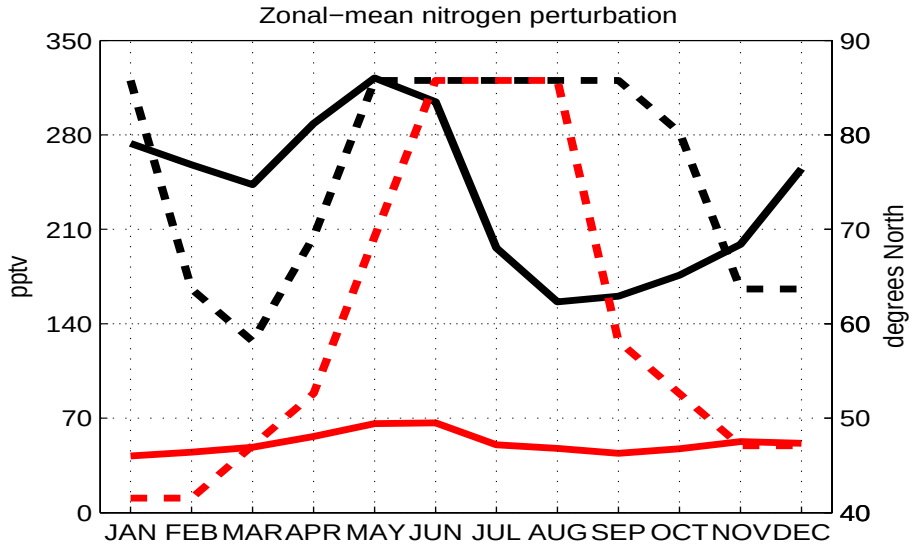

Fig. 5. Maximum increase in monthly averaged zonal-mean NO_y (black) and NO_x (red) due to aircraft in the TRADEOFF reference case as a function of season, i.e. 'yy minus 00'. Solid lines: magnitude of the maximum (pptv, left axis), dashed lines: latitude at which the maximum increases occur (degrees North, right axis).

ACPD
5, 12255–12311, 2005

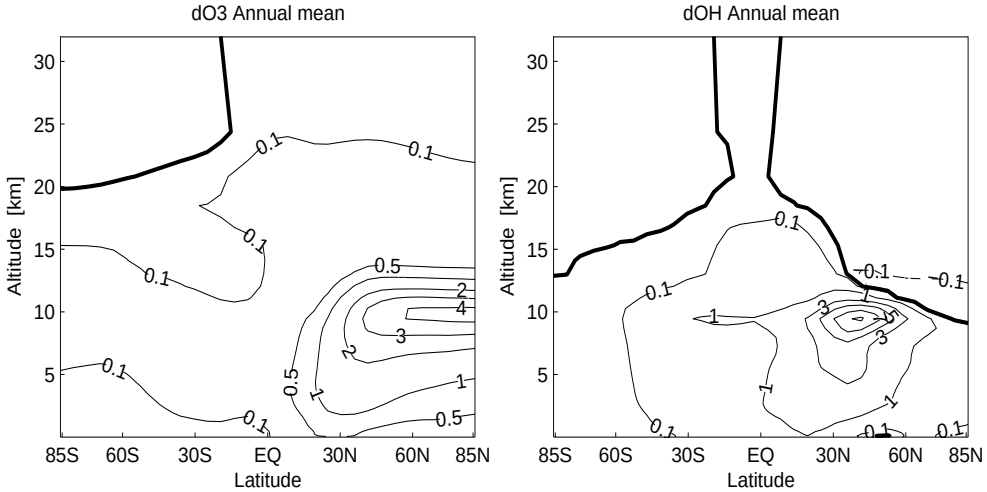

Fig. 6. Annually averaged changes in zonal-mean ozone (ppbv) and OH (10^4 molecules cm^{-3}) due to aircraft emissions in the TRADEOFF reference case, i.e. 'yy minus 00'. Contours at: −0.1, 0, 0.1, 0.5, 1, 2, 3, 4 for ozone and −1, −0.1, 0, 0.1, 1, 3, 5, 7, 9 OH.

ACPD
5, 12255–12311, 2005

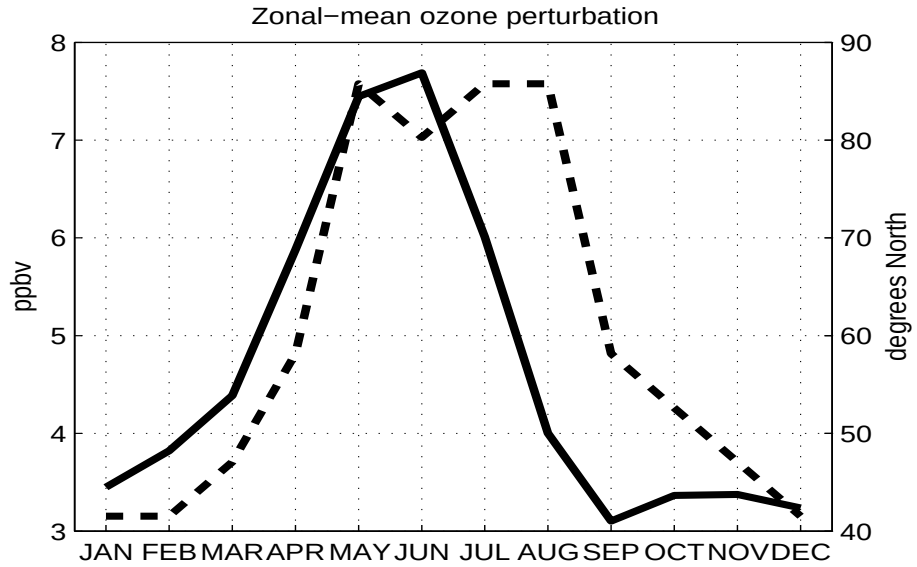

Fig. 7. Maximum increase in monthly averaged zonal-mean ozone due to aircraft in the TRADEOFF reference case as a function of season, i.e. 'yy minus 00'. Solid line: magnitude of the maximum (ppbv, left axis), dashed line: latitude at which the maximum increase occurs (degrees North, right axis).

ACPD
5, 12255–12311, 2005

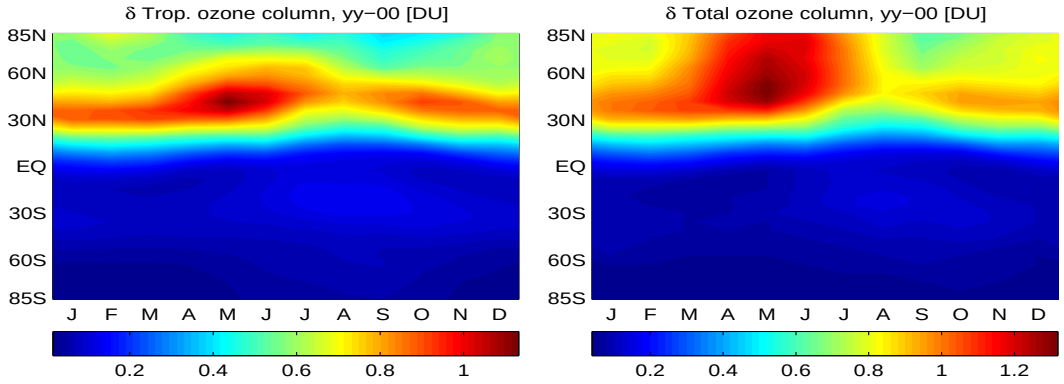

Fig. 8. Changes in the tropospheric (left panel) and total (right panel) ozone columns due to aircraft emissions in the TRADEOFF reference case, i.e. 'yy minus 00' (units: DU).

ACPD
5, 12255–12311, 2005

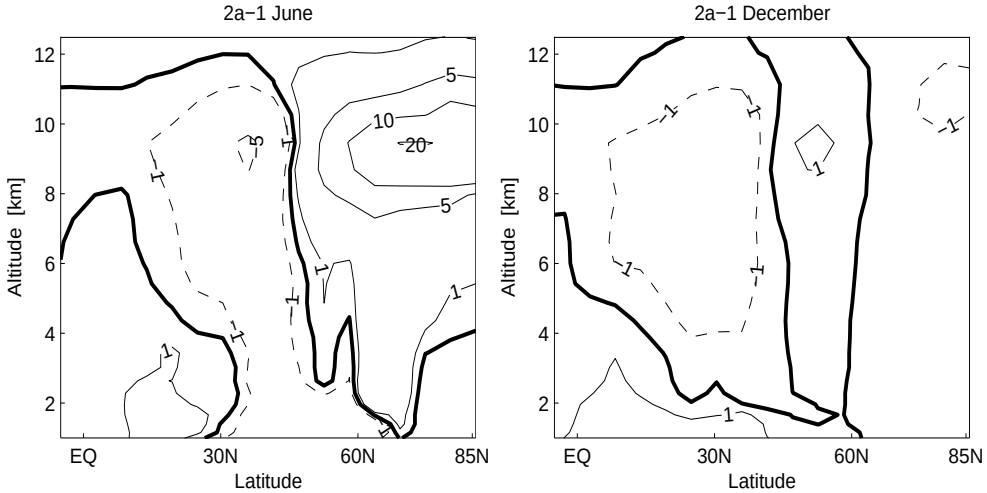

Fig. 9. Change in net chemical ozone production (10^3 molecules cm^{-3} s^{-1}) due polar routes replacing conventional routes, i.e. '2a minus 1' in June (left) and December (right). Contours at −5, 1, 0, 1, 5, 10, and 20.

ACPD
5, 12255–12311, 2005

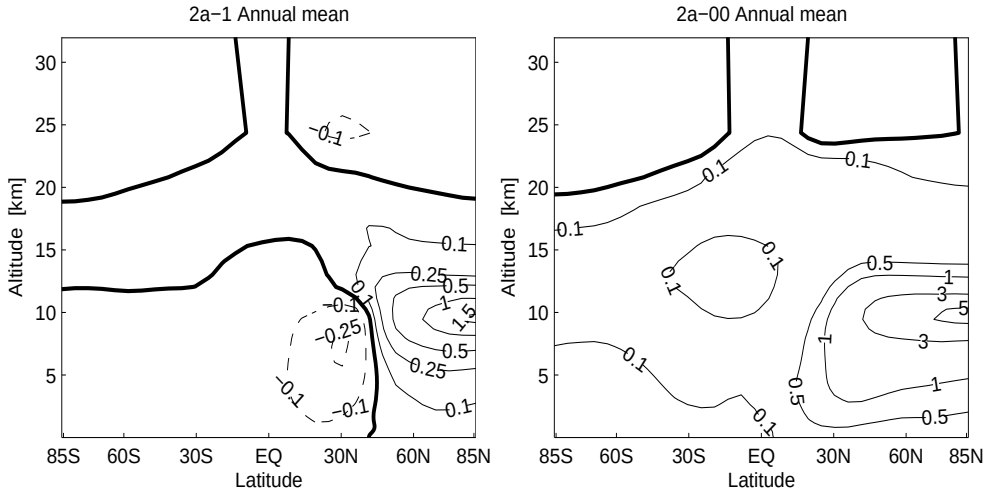

Fig. 10. Annually averaged zonal-mean ozone change (ppbv) due to polar routes replacing conventional routes (left panel, '2a minus 1') and the total impact due to aircraft emissions in the normalized polar route scenario (right panel, '2a minus 00'). Contours at −0.25, −0.1, 0, 0.1, 0.25, 0.5, 1, 1.5, 3, and 5 (in the right panel the 0.25 and 1.5 contours are omitted).

ACPD
5, 12255–12311, 2005

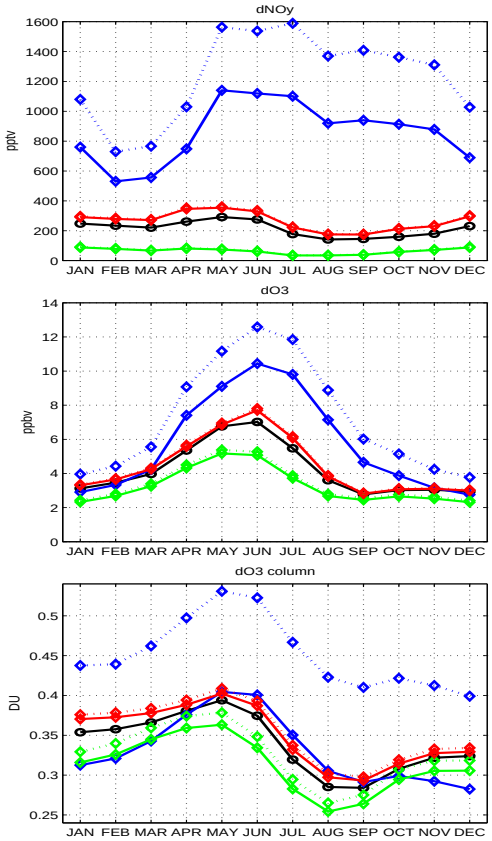

Fig. 11. Maximum zonal-mean NO_y increase (upper panel, pptv), maximum zonal-mean ozone increase (middle panel, ppbv), and globally averaged ozone column increase (bottom panel, DU) as a function of season for different TRADEOFF simulations with respect to the 'no aircraft' run. Solid black line: '1 minus 00', solid blue line: '2a minus 00', dotted blue: '2b minus 00', solid green: '3a minus 00', dotted green: '3b minus 00', solid red: '5a minus 00', dotted red: '5b minus 00'.

ACPD
5, 12255–12311, 2005

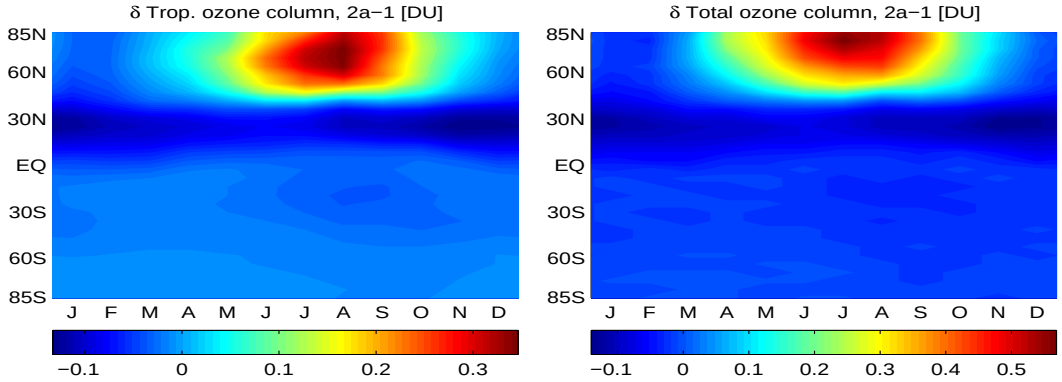

Fig. 12. Changes in the tropospheric and total ozone columns (DU) due to polar routes replacing conventional routes ('2a minus 1').

ACPD
5, 12255–12311, 2005

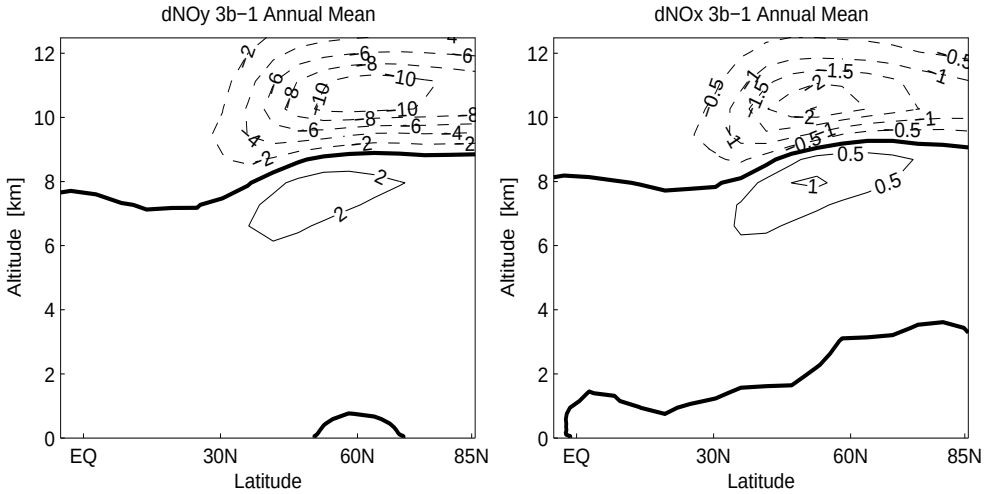

Fig. 13. Annual-mean changes in concentrations of NO_y (top left, 10^8 molecules cm^{-3}) and NO_x (top right, 10^8 molecules cm^{-3}) in the Northern Hemisphere due to a 1830 m reduction in flight altitude taking into account changes in fuel consumption, i.e. '3b minus 1'. Contours at −12, −10, −8, −6, −4, −2, 0, 2 for NO_y and −2.5, −2, −1.5, −1, −0.5, 0, 0.5, 1 for NO_x.

ACPD
5, 12255–12311, 2005

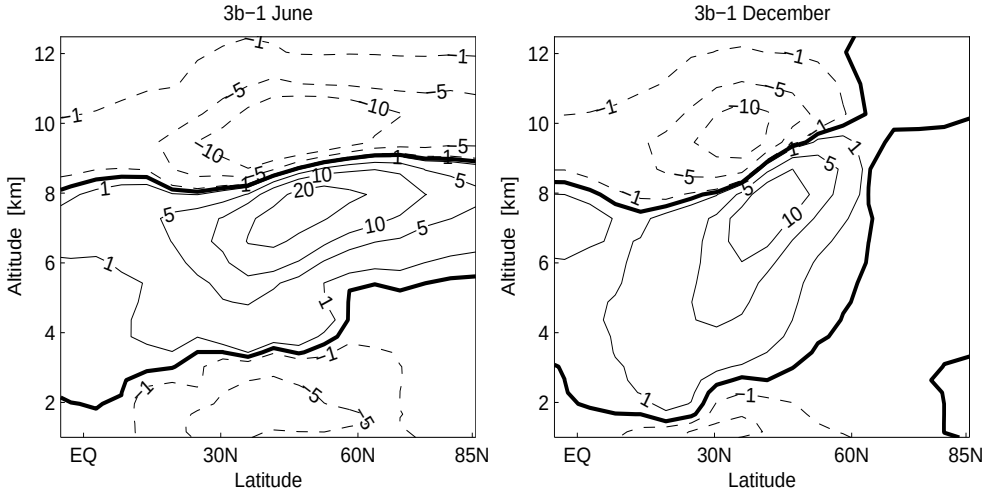

Fig. 14. Change in net chemical ozone production (10^3 molecules cm^{-3} s^{-1}) due to a 1830 m reduction in flight altitude, taking into account changes in fuel consumption, i.e. '3b minus 1' in June (left) and December (right). Contours at −20, −10, −5, −1, 0, 1, 5, 10, and 20.

ACPD
5, 12255–12311, 2005

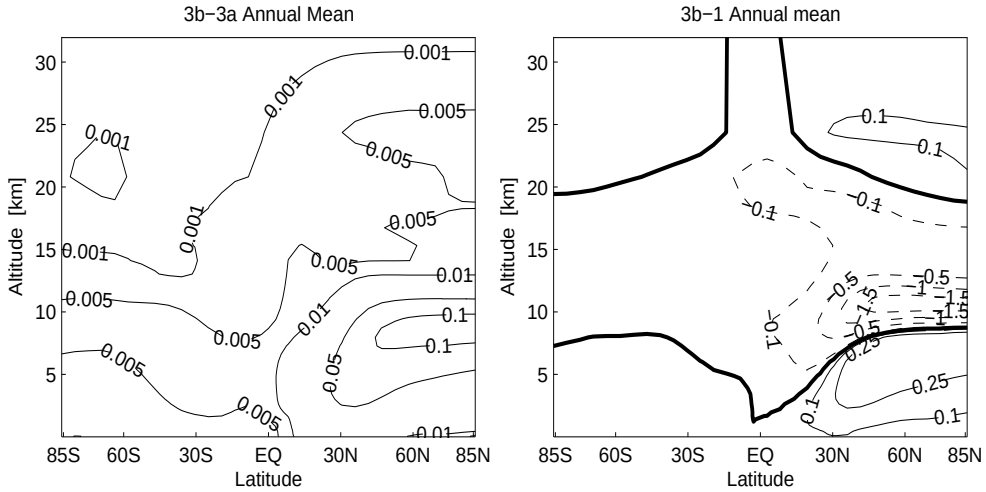

Fig. 15. Annually averaged zonal-mean ozone change (ppbv) due a 1830 m reduction in flight altitude. Left panel: '3b minus 3a', i.e. separated effect of changes in fuel consumption, and right panel: '3b minus 1', i.e. total effect of lowering the flight altitude.

ACPD
5, 12255–12311, 2005

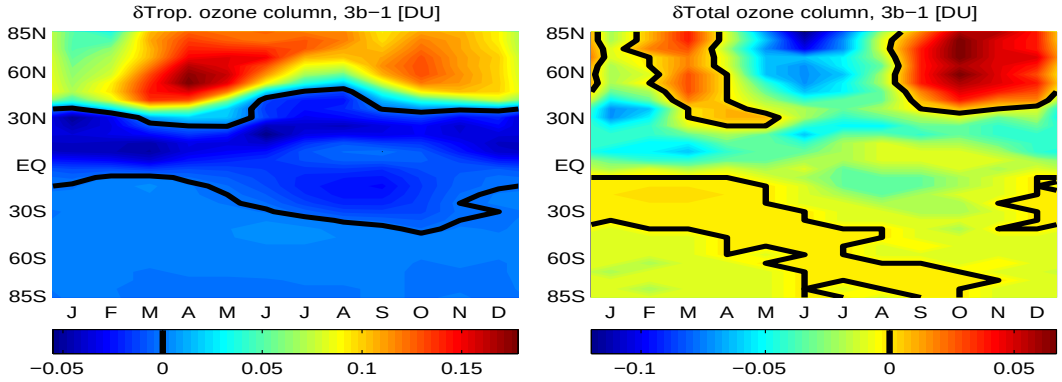

Fig. 16. Changes in the tropospheric and total ozone columns (DU) due to a 1830 m reduction in flight altitude, taking into account changes in fuel consumption ('3b minus 1').

ACPD
5, 12255–12311, 2005

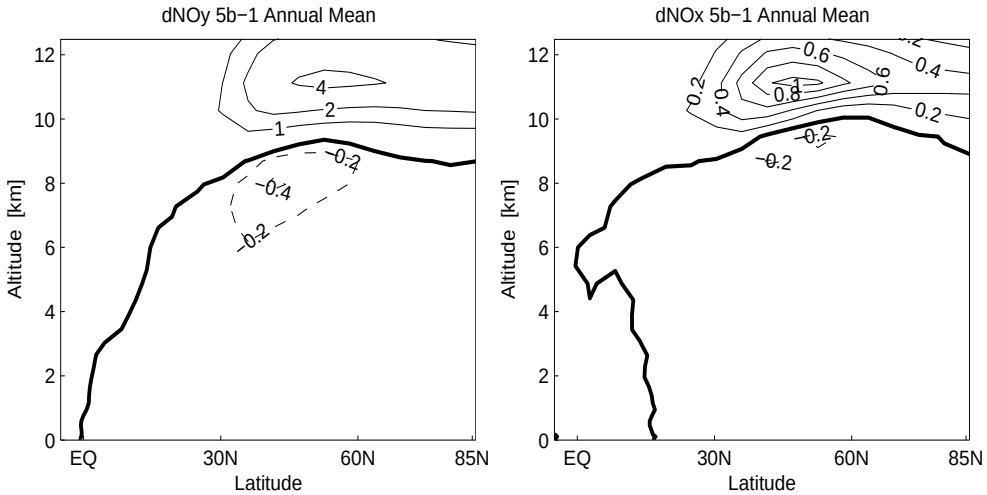

Fig. 17. Annual-mean changes in concentrations of NO_y (top left, 10^8 molecules cm^{-3}) and NO_x (top right, 10^8 molecules cm^{-3}) in the Northern Hemisphere due to a 610 m increase in flight altitude taking into account changes in the total emission of nitrogen, i.e. '5b minus 1'. Contours at −0.4, −0.2, 0, 1, 2, 4 for NO_y and −0.4, −0.2, 0, 0.2, 0.4, 0.6, 0.8, 1.0 for NO_x.

ACPD
5, 12255–12311, 2005

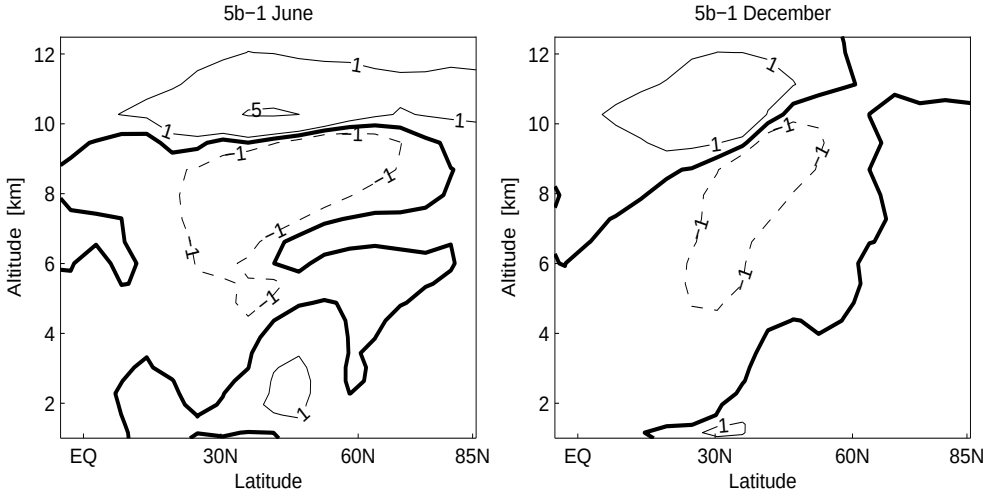

Fig. 18. Change in net chemical ozone production (10^3 molecules cm^{-3} s^{-1}) due to a 610 m increase in flight altitude, taking into account changes in the total emission of nitrogen, i.e. '5b minus 1' in June (left) and December (right). Contours at −5, −1, 0, 1, 5.

ACPD
5, 12255–12311, 2005

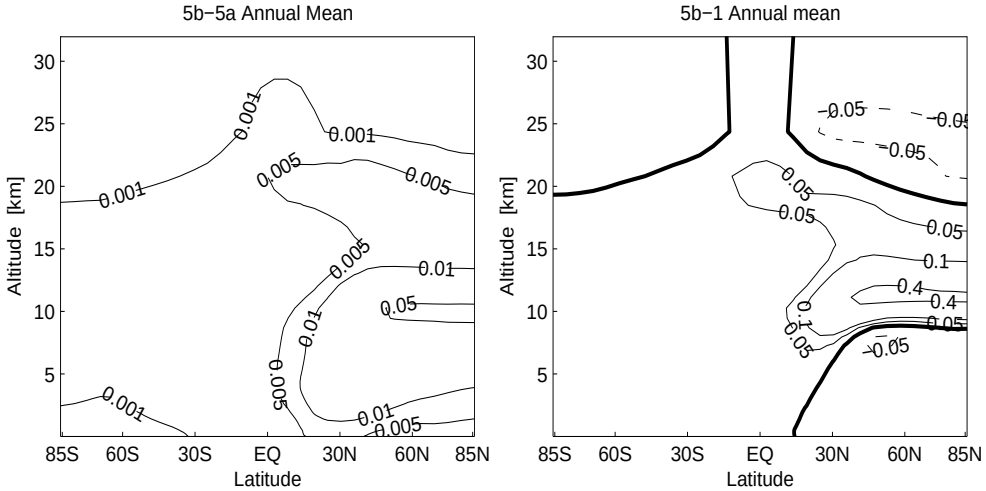

Fig. 19. Annually averaged zonal-mean ozone change (ppbv) due a 610 m increase in flight altitude. Left panel: '5b minus 5a', i.e. separated effect of changes in fuel consumption, and right panel: '5b minus 1', i.e. total effect of increasing the flight altitude.

ACPD
5, 12255–12311, 2005

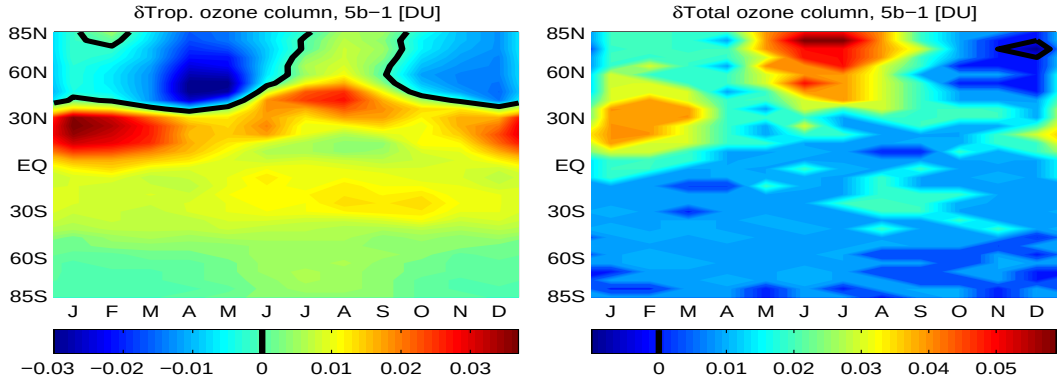

Fig. 20. Changes in the tropospheric and total ozone columns (DU) due to a 610 m increase in flight altitude, taking into account changes in fuel consumption ('5b minus 1').

ACPD
5, 12255–12311, 2005

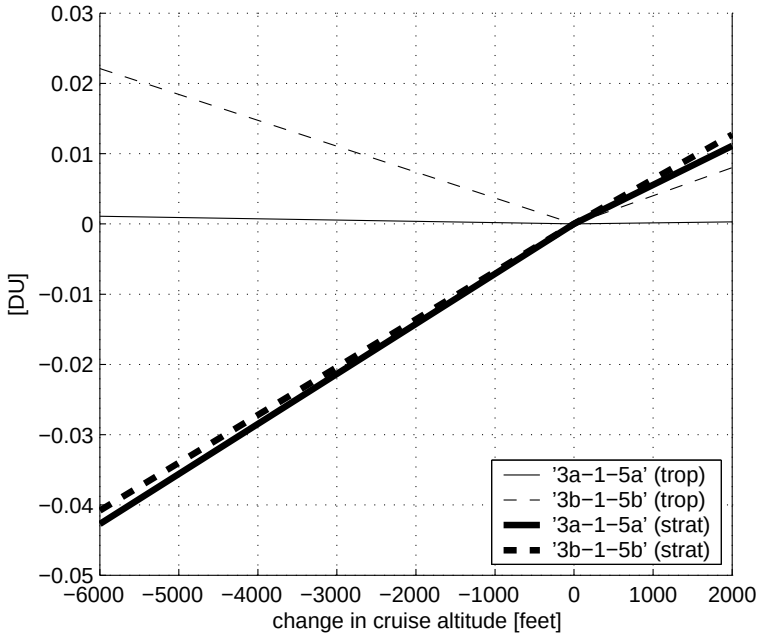

Fig. 21. Change in the Northern Hemisphere average tropospheric and stratospheric ozone columns (DU) due to changes in flight altitude, based on the numbers given in Table 4. The increase in the base case run '1' is set to zero. E.g., the thin dashed line depicts the 0.0221 DU increase in tropospheric ozone column in simulation '3b' with respect to '1' (at −6000 feet) and the 0.0080 DU increase in the tropospheric ozone column in simulation '5b' with respect to '1' (at +2000 feet).

ACPD

5, 12255–12311, 2005